AD

USAAVLABS TECHNICAL REPORT 65-65

AIR LOADINGS ON A ROTOR BLADE AS CAUSED BY TRANSIENT INPUTS OF COLLECTIVE PITCH

By

L. Segel

October 1965

U. S. ARMY AVIATION MATERIEL LABORATORIES
FORT EUSTIS, VIRGINIA

CONTRACT DA 44-177-AMC-77(T)
CORNELL AERONAUTICAL LABORATORY, INC.

DEPARTMENT OF THE ARMY
U. S. ARMY AVIATION MATERIEL LABORATORIES
FORT EUSTIS, VIRGINIA 23604

This report has been reviewed by the U. S. Army Aviation Materiel Laboratories and is considered to be technically sound. It is published for the exchange of information, the stimulation of ideas, and application as may be appropriate.

Task 1P125901A142
Contract DA 44-177-AMC-77(T)
USAAVLABS Technical Report 65-65
October 1965

AIR LOADINGS ON A ROTOR BLADE AS CAUSED BY TRANSIENT INPUTS OF COLLECTIVE PITCH

CAL Report BB-1840-S-1
by

L. Segel

Prepared by

Cornell Aeronautical Laboratory, Inc.
Buffalo, New York

for

U. S. ARMY AVIATION MATERIEL LABORATORIES
FORT EUSTIS, VIRGINIA

SUMMARY

A method is developed for predicting the nonperiodic air loads caused by control inputs applied to a rotary wing in forward flight. Use is made of a numerical description of the geometry and circulation strength of the vorticity in the wake to compute the time-varying, nonuniform-flow field in the plane of the rotor disc. The method of approach is similar to that developed previously for the steady-state flight condition, the major difference being that the solution procedure lends itself to the treatment of transient phenomena, such as the nonperiodic loadings caused by time-varying collective pitch.

Several approximations are made to simplify the analysis. The major assumptions are: (1) the rotor blades are structurally rigid and have only a flapping degree of freedom; (2) the hub of the rotor continues to translate in level, constant-speed flight during the short time interval of interest; (3) the geometry of the wake can be specified a priori; and (4) no account need be taken of the shed vorticity in the wake.

Computed flapping and air load distributions are compared with transient data obtained in wind-tunnel tests on a full-scale H-34 rotor. In general, very encouraging agreement is found leading to the conclusion that calculation and prediction of nonperiodic loadings on rotary wings is a feasible task.

FOREWORD

This investigation of air loadings on rotary wings was conducted at the Cornell Aeronautical Laboratory, Inc. (CAL), under U. S. Army Contract DA 44-177-AMC-77(T) during the period September 1963 through May 1965. The program was sponsored by the U. S. Army Aviation Materiel Laboratories (USAAVLABS), Fort Eustis, Virginia, as Task 1P125901A142, and was administered by Mr. J. E. Yeates.

Mr. Leonard Segel is the project engineer and author of this report. He was aided in a very large measure by Mr. Edwin F. Chmielewski of the Computer Services Department (CAL) who performed the monumental task of generating a working computing-machine program. Acknowledgement is also made of the combined efforts of personnel from the Ames Research Center, National Aeronautics and Space Administration and Sikorsky Aircraft Division, United Aircraft Corporation, in providing the experimental data used to validate the analysis.

CONTENTS

ILLUSTRATIONS

LIST OF SYMBOLS

JSG	Blade segment number for maximum circulation
I_b	Moment of inertia of blade about flap hinge, slug-ft ^{2}
LCN	Number of spanwise blade segments
M_a	Moment about flapping hinge caused by aerodynamic loading, ft/lbs
$MBLM$	Azimuth index limit for nonrolled wake
M_w	Weight moment of blade, ft/lbs
NA	Number of azimuth positions per rotor revolution (an integral multiple of NB)
NB	Number of blades
NR	Number of revolutions of wake
R	Rotor radius, ft
T	Aerodynamic loading at blade load point, lbs/ft
U_p	Component of air velocity relative to the blade (at the three-quarter chord position) in a plane containing the blade-span axis and the rotor axis and oriented perpendicular to the blade span, ft/sec
U_T	Component of air velocity relative to the blade, perpendicular to the plane containing the blade-span axis and the rotor axis, ft/sec

V	Forward flight velocity, ft/sec
X, Y, Z	Shaft axis system with origin located at rotor hub (see Figure 6)
a	Lift curve slope $\left(\frac{dC_l}{d\alpha}\right)$, nondimensional
b	Blade semichord, ft
e	Radial distance from rotor axis to blade root, ft
g	Gravitational acceleration, ft/sec ^{2}
$\dot{h}$	"Effective plunging" velocity of the three-quarter chord point of a specified segment on a rotor blade, ft/sec
i	An index designating a blade on a rotary wing
ib	An index designating the wake trailed by blade
j	An index designating a spanwise position on a rotor blade
k	An index designating a spanwise position in the wake
l_a, m_a, n_a	Components, along the x, y, z axes, respectively, of the position vector between the "forward" end of a wake element and a load point on the blade, ft
l_b, m_b, n_b	Components, along the x, y, z axes, respectively, of the position vector between the "aft" end of a wake element and a load point on the blade, ft
m	An index designating an instant of time

$\bar{m}$	An index designating an azimuthal position in the wake
r	Radial distance from center of rotation to midpoint of blade segment, or to other specified point, ft
$\bar{r}$	Radial distance from rotor axis to end point of blade segment, ft
$\bar{\bar{r}}$	Radial distance from rotor axis to spanwise location of rolled-up root and tip vortex, ft
r_a, r_b	Length of position vector between a load point and the forward and aft ends, respectively, of a wake element, ft
r/R	Nondimensional radial distance from rotor axis to specified point on a blade
u, v, w	x, y, z components of velocity induced by the wake at a specified point on a blade, ft/sec
$\bar{w}$	Mean induced downwash governing the vertical transport of vorticity in the wake, ft/sec
w_T	z component of velocity induced by all elements of the wake other than the trailing elements adjacent to the blades
x, y, z	A "wind" axis system with the origin located at the hub of the rotor (see Figure 6)
Γ	Circulation, either bound or trailing, ft^2/sec
Ω	Angular velocity of rotor shaft, rad/sec
α	Angle of attack at specified blade segment, rad
α_s	Shaft angle of attack (positive for forward tilt of the rotor shaft), rad

β	Flap angle of blade relative to plane normal to rotor shaft, rad
ϵ	Flap hinge offset, ft
θ	Pitch angle of a given blade segment (as measured in a shaft axis system), rad
θ_0	Collective pitch setting of rotor (reference is at the rotor axis) rad
θ_{1c}	Cosine cyclic pitch, rad
θ_{1s}	Sine cyclic pitch, rad
$\Delta\theta/R$	Blade twist (linear), rad/ft
ξ, η, ζ	Coordinates of endpoints of trailing vorticity as measured in the x, y, z axis system, ft.
σ	Influence coefficient yielding induced velocity at a specified point as caused by an element of vorticity of unit strength, 1/ft
φ	Angle between air velocity vector relative to the blade and the rotor shaft plane, rad
ψ	Azimuth angle ($\psi = 0$ when blade is oriented along positive x axis), rad

NOTE: A single dot over a variable denotes the first time derivative; a double dot denotes the second time derivative.

INTRODUCTION

The design of rotor blades to tolerate the oscillatory stresses encountered by a helicopter in forward flight is recognized as one of the major problems facing the designers of helicopter rotor systems. This problem, together with the requirement for improving the structural integrity of rotary wings, has necessitated the development of research programs whose objective is the derivation of rational and valid procedure for predicting the time-varying air loadings and stressing of rotor blades designed for helicopter applications. Since the problem is worldwide, research has been and is being performed in a number of countries. The VTOL Dynamic Loads Symposium held in June 1963 under the joint sponsorship of the Cornell Aeronautical Laboratory, Inc. (CAL) and the U. S. Army Aviation Materiel Laboratories (USAAVLABS) gave evidence of the effort being mounted both in the United States and abroad.

It is now recognized that the crux of the helicopter blade-load prediction problem is the requirement to model the airflow through the rotor in considerably more accurate detail then has been sufficient heretofore for studies of rotor performance. To this end, investigators such as Willmer [1], Molyneux [2], Miller [3, 4, 5], Tararine [6], Shi-Tsun [7, 8], Davenport [9], DuWaldt and Piziali [10, 11] have developed mathematical models of the rotor-wake system (in a variety of formats) for the purpose of predicting the air loadings produced in steady, forward flight. It appears that these investigations can, in part, be differentiated from one another by the extent to which resort is had to high-speed computing machinery in order to minimize the necessity for simplifying the mathematical treatment.

The investigation reported herein is an extension of the rotor-wake modeling concepts previously described in Reference 12. This extension consists primarily in the recasting of the original analysis that was suitable for steady-state calculations to one that yields a temporal and spatial history of the pertinent response variables as a function of time-varying changes in collective pitch. Accordingly, reference shall be made throughout this report to "steady-state blade loads" (SSBL) calculations and to "transient blade loads" (TBL) calculations.

It should be understood that the SSBL calculation (as described in Reference 12) consists of a procedure wherein the instantaneous velocities induced by the wake of the rotor are determined for each blade section in a rotating coordinate system. Further, the SSBL model of wake vorticity results in an inflow distribution that varies with time and position in the rotor disc, but which is periodic with each revolution of the rotor thus producing an integrated mean value of inflow that does not change with time. Thus, we use the term "steady state", even though the inflow seen by a blade section is varying continually during one revolution of the rotor.

On the other hand, a TBL calculation must consist of a procedure wherein nonperiodic induced velocities and loadings can be determined. When collective blade-pitch control is applied, such as to change the mean thrust being produced by a rotor, the momentum that is imparted to the air mass by the rotor must be changed. This is to say that the air mass must be accelerated until a new steady-state thrust corresponding to the changed operating conditions is achieved. From the point of view of momentum theory, a time interval must elapse during which the air mass associated with a rotor is accelerated to its new steady state inflow velocity. From the microscopic point of view, wherein inflow is viewed as being induced by wake vorticity, additional time rates of change of inflow are created by the existence of a wake of vortex filaments and strengths that are no longer periodic with respect to one revolution of the rotor. Thus, there is an equivalence between the momentum concept of an air mass being accelerated during the transient interval between two steady states and the concept in which a change in vorticity level is diffused through the wake bringing about a change in the velocities induced at the rotor disc by the wake.

Other investigators [13, 14] have measured the response of a hovering or vertically-moving rotor to a change in collective pitch. They found that the thrust response was highly sensitive to the rate of change of collective pitch for rapid control inputs and were able to explain the measured results in terms of the requirement to accelerate an apparent additional mass of air associated with a rotor considered to be an impervious disc. Although the concept of additional mass may suffice to relate the time-varying total thrust on a blade or rotor to a time variation in blade pitch, this concept is not suitable for computing the inflow distribution required to determine blade loadings as a function of spanwise location, azimuth position, and time. Rather it is necessary to compute the inflow caused by a wake possessing elements of vorticity whose strengths vary in a nonperiodic fashion as a result of a time-varying change in collective pitch. It is this particular task that consituted the major objective of this investigation. Successful accomplishment of this task is viewed as a first and major step towards computing the detailed temporal and spatial distribution of aerodynamic loads encountered by a helicopter rotor during maneuvering flight.

Earlier analyses of transient air loads on rotary wings are reviewed in the report prior to presenting the analytical approach developed for purposes of modeling TBL phenomena. The presentation of the method of approach used in this investigation includes a discussion of rotor-wake representation and a brief description of the developed computational procedure. This description is followed by a comparison of theoretical calculations and experiment, with the technical discussion being concluded by presenting both the current capabilities and shortcomings of the developed analytical procedure, as applied to specific flight regimes. Details pertaining to the developed mathematical model and computational procedure are given in an appendix.

CONCLUSIONS

This investigation has shown that the prediction of nonperiodic air loadings on rotary wings is a feasible task. Although the agreement achieved between theory and experiment indicates that the major aspects of transient blade loading phenomena are adequately represented in the analysis, future refinements of the existing mathematical model will be required to provide a prediction capability having a high order of accuracy. Ultimately, it should prove possible to use the TBL calculation procedure to investigate almost any rotor dynamics problem wherein it is necessary to include an adequate description of the wake-induced flow field. This work should be looked on as a first step towards the goal of computing the air loadings on the rotor of a maneuvering helicopter.

It is further concluded that:

(1) A wake model consisting only of trailing vortex elements, trailed as a consequence of a spanwise variation in bound vorticity, constitutes a first-order representation of the wake of a rotary wing.

(2) The radial contraction of the rolled-up root and tip vortices of a rotary wing must be simulated in order to obtain accurate predictions of the air load distribution produced in hovering flight. It would appear that this conclusion also holds for forward flight at very small advance ratios.

(3) For the limiting case of steady forward flight, the TBL computational procedure provides results which are equivalent to those yielded by the previously developed SSBL calculations. Identical steady periodic air loadings are predicted by both procedures provided the tip-path-plane orientation predicted by the TBL procedure is in agreement with the orientation specified in the SSBL calculation. As a result of the integration performed in the TBL calculation to obtain the total lift on the rotor, it was observed that nonuniform-inflow calculations yield an oscillatory four-per-revolution component of total shear at the hub having an amplitude of 0.1 g (approximately) in all cases studied for the H-34, whereas uniform-inflow calculations yield very little oscillatory component in the total shear transmitted to the rotor hub.

(4) The aerodynamic model, in its present form, together with a model of the kinematics and dynamics of a flapping degree of freedom, yields flapping and air loading responses

caused by a change in collective pitch that are in good agreement with wind tunnel measurements made on a full-scale H-34 rotor.

(5) Preliminary and tentative support has been obtained for a hypothesis stating that a wake assumed to have a constant strength corresponding to the mean total load on a rotor would produce a reasonable approximation of the velocity field that is induced in the plane of the rotor disc. A considerable number of computational studies is required to place this hypothesis on a firmer foundation.

(6) Although the wake spacing (i.e., wake pitch) assumed to exist in the steady state preceding and following a transient interval has a significant influence on the steady total load and load distribution achieved in hover, the timewise variation of loading does not appear to be a highly sensitive function of the manner in which the wake spacing is assumed to vary during the transient interval. Since loadings produced in forward flight do not appear to be very sensitive to small variations in the assumed value of the vertical transport velocity, it appears that the question of how and when the wake spacing changes during the transient interval is not crucial to the task of making reasonable predictions of transient air loadings. This conclusion holds only for the range of conditions studied, namely, maximum advance ratio and maximum change in collective pitch equal to 0.287 and 2.7 degrees respectively, and may not be valid for more severe maneuvers or higher advance ratios.

(7) Two deficiencies of the developed TBL model discovered in the process of conducting this study are the assumptions that (1) the trailing vortices trail free from the one-quarter chord and (2) maximum circulation on a rotor blade occurs at a specific spanwise position on the blade. Calculations have shown that the former assumption leads to computational difficulties whenever the control point in a given spanwise segment falls outside the horseshoe vortex associated with that segement. With respect to the second assumption, results computed for certain flight conditions demonstrate that the location of maximum circulation shifts markedly along the span with changing azimuth and, accordingly, the program, as presently constituted, assigns incorrect circulation strengths to the rolled up tip and root vortices. These problems can be eliminated, respectively, by trailing vorticity from the trailing edge of the blade and using program logic that seeks out the maximum circulation for assignment to the rolled-up wake.

RECOMMENDATIONS

The demonstrated ability for computing both periodic and nonperiodic air load distributions on rotary wings holds forth the promise of, ultimately, being able to compute (1) the performance, (2) the maneuver response, (3) the vibratory loading and stresses, and (4) the response to gust disturbances as modified and controlled by the spiral wake that is peculiar to the rotary wing. It should be noted that this "promise" appears to be more constrained by practical limitations on the development of suitable computing procedures rather than by inherent limitations on the development of a mathematical analog of the phenomenon. Accordingly, it is recommended that continuing investigations of the dynamics of rotary wings pay particular attention to eliminating unnecessary details in the simulation while seeking to incorporate those refinements in the theory essential to obtaining improved agreement between prediction and measurement.

Although many different approximations have been made in the development of the TBL computational model, they may be grouped in three general categories: (1) aerodynamic simplifications, (2) wake-modeling simplifications, and (3) blade-structure and rotor-kinematics simplifications. Questions still remain as to which of these three categories of simplifications constitute the primary source disagreement currently being obtained between prediction and measurement. Accordingly, it is recommended, that wherever possible, improvements in the computational model be made sequentially in order to assess the degree to which a given change in the model influences its level of accuracy. It is reemphasized that this recommendation is motivated by a strong appreciation for the programming difficulties and, more importantly, the computing time and costs that are associated with predictions of SSBL and TBL phenomena.

The logical extension to the analysis reported herein would be the introduction of additional degrees of freedom such that blade loadings and motions in the flapwise, pitchwise, and edgewise directions, together with the angular velocity response of the rotor, can be predicted as a function of transient inputs of blade pitch and/or shaft torque. The research objective recommended for this study would be the determination of transient response characteristics of a rotary wing as influenced by (1) the peculiar blade-wake relationships that exist or (2) the inertial and/or aerodynamic coupling forces and moments that prevail during the transient interval associated with changes in blade-pitch control or changes in mechanical torque applied to the rotor shaft. In the latter instance, the generated mathematical model would serve as a means for gaining additional insight into the dynamics of rotors following a power failure, for example. Ultimately, consideration could and should be given to including shaft and fuselage degrees of freedom in a TBL model for purposes of investigating the extent to which improved performance and stability and control analyses can be made as a result

of eliminating the traditional assumption of uniform inflow. Mention should also be made of the urgent requirements for performing research that will define the aerodynamic behavior of rotors at very high or infinite advance ratios. Specifically, the high advance ratios to be attained by compound and stoppable-rotor helicopter designs will cause rotor blades to encounter flow conditions in which existing methods of aerodynamic analysis are no longer valid.

PRIOR STUDIES OF TRANSIENT AIR LOADS ON ROTARY WINGS

Of the total literature dealing with the transient loadings experienced by rotary wings, only that portion in which efforts are made to derive predictive analytical models are of concern here. A review has shown that in every case in which analytical predictions of transient loadings have been made, these predictions have dealt with the integrated behavior of the rotor rather than with "microscopic" detail, namely, the time and space distribution of induced velocity and the resulting air loadings.

The efforts of Carpenter and Fridovich [13] and Rebont, et al, [14] (as mentioned in the Introduction) are particularly worthy of mention. In the first work, equations were developed to predict the thrust, induced velocity, and flapping response of a rotor to a rapid increase of blade pitch. A combination of blade-element theory and the momentum theory was used, with the momentum equations modified to apply to a transient condition where the inflow is being accelerated. This modification was implemented by considering the mass of air being accelerated to be equal to the "apparent additional mass" of fluid associated with an accelerating impervious disc. The set of equations yielding the desired representation of the selected physical phenomenon were as follows:

(1) Instantaneous thrust yielded by blade-element theory equated to the instantaneous thrust yielded by modified momentum theory.

(2) The flapping-motion equation, with blades assumed rigid.

(3) The helicopter motion or lift equation.

Experiments performed on a test tower yielded results which were compared with computed solutions of the first two equations, the third equation not being needed since the vertical velocity of the hub was zero due to its fixed position. The concept of apparent additional mass appeared to account satisfactorily for the measured average inflow and thrust response to change in collective pitch.

The second study [14] was similar to the investigation described above. This latter investigation was concerned with the response to a change in collective pitch in descending flight (near the autorotation regime) whereas the former study was concerned with vertical takeoff, i. e., with zero vertical velocity and zero thrust for the initial conditions. The concept of apparent mass was similarly employed to modify the momentum equation to yield instantaneous values of thrust. Flapping was neglected and the blade-element thrust was combined with

momentum thrust to yield a differential equation having the form of Riccati's equation. With collective pitch given as a known function, the resulting equation was numerically integrated for a range of rotor operating conditions yielding results that bear some resemblance to those obtained by Carpenter and Fridovich. Data obtained in experiments appeared to verify (qualitatively) predictions made for various nondimensional rotor parameters; however, these investigators concluded that the apparent mass defined by Carpenter and Fridovich should be doubled in order to account satisfactorily for their experimental results. Both groups of investigators showed that the thrust response is highly sensitive to the rate of change of the collective pitch.

Michel, et al, [15] used the principle of superposition to separate the response of a helicopter to a gust from the periodic response that exists for an articulated rotor in forward flight. Equations and solution techniques were developed to yield the transient response of a rotor upon entering a sharp-edged gust. Aerodynamic loadings were computed on the basis of a time invariant, uniform inflow. It should be noted that this study was concerned with procedures yielding overall gust load or alleviation factors rather than with the details of blade loading, blade motion, and blade stress. A subsequent investigation [16] constituted an experimental check on these theoretical results and demonstrated order of magnitude agreement between theory and experiment. The experimental results indicated, however, that the blade flapping and moment response is influenced by the collective pitch setting of the rotor, in contrast to the assumption made in the analysis [15], namely, that the gust response is independent of the steady-state periodic response that exists in forward flight.

Except for the absence of means for computing the detailed influence of a vortical wake, Gessow and Crim [17] developed a computing program (in 1955) that bears a close resemblance to the program developed in the investigation reported herein. This reference is cited last since it represents the state of the art prior to the present study for computing the transient flapping of helicopter rotor blades. In fact, the procedure as developed by Gessow and Crim (or modified form) is currently employed by the helicopter industry to compute both the steady-state and transient flapping behavior of rigid-blade rotors. The computational procedure is employed mainly for (1) investigating questions of rotor stability at high advance ratios, (2) determining steady-state, tip-path-plane orientations, and (3) predicting performance characteristics. Provision is generally made for determining blade thrust as a function of lift and drag data obtained from two-dimensional airfoil tests over a zero-to-360-degree range of angle of attack. However, no provision is made for introducing the influence of temporal and spatial variations in induced velocity, since such variations require that a suitable mathematical model of a rotor wake be available.

It should be again pointed out that the present study is primarily concerned with the elimination of the traditional assumption of uniform inflow such that the impulsive and/or high frequency components of blade loading due to the presence of the spiral, vortical wake can be determined with reasonable accuracies. Previous research efforts [12] have demonstrated that this objective can be achieved for SSBL calculations, albeit at the cost of considerable program complexity and computing time.

REPRESENTATION OF THE ROTOR WAKE

GENERAL REMARKS

For purposes of computing the transient air loadings caused by changes in collective pitch, the rotor and its wake are modeled (mathematically) in essentially the same format that was adopted for the SSBL calculations described in Reference 12. Namely, each blade of the rotor is represented by a segmented lifting line (bound vortex) located along the quarter chord of the blade, and the wake is represented by a mesh (or lattice work) of segmented, straight vortices, with the strength of the vortex being constant over the length of the segment. Whereas, previously, the wake was considered to consist of a large number of closed "boxes" of vorticity, constituting a convenient means for "lumping" the distributed vorticity in the wake into discrete elements of shed and trailing vorticity, the wake adopted for the TBL model is assumed to consist only of trailing elements. Omission of the shed elements means that we have elected to ignore the influence of unsteady aerodynamics (associated with the changing circulation on a two-dimensional segment of the rotor blade) in computing air loadings in the TBL calculation. This simplifying assumption was adopted as a result of (1) having performed a study of means for simplifying the wake model (which study will be described below), (2) recognizing that theoretical means for including unsteady aerodynamic effects in the TBL model are not clearly established, and (3) the large motivation that exists for reducing the complexity of the wake calculations whenever it appears to be reasonably justifiable. A most important feature of the wake model that has been employed heretofore for making calculations of air loadings on rotary wings is the requirement to specify beforehand the gross geometry of the vortex elements in the wake. In practice, this has meant that the steady-state wake is treated as a "rigid" wake in which the pitch of the spiral is determined by a "transport" velocity equal to the mean velocity induced by the rotor, as yielded by momentum theory. A transient wake, equivalent to the rigid wake produced in steady, forward flight, is one in which the vorticity is trailed from a blade executing nonperiodic rather than periodic motions in space. Note that a tip-path-plane is not defined. However, the vorticity, subsequent to being trailed by the blade, acquires a geometry governed by a priori statements about the steady and time-varying components of the velocity transporting the vorticity in a direction perpendicular to the horizontal line of flight.

This a priori specification of the time-varying transport velocity greatly simplifies the model of a rotor-wake system. In so doing, we eliminate the necessity to compute the self-induced effects of the wake, either in terms of how these self-induced effects control (1) the "steady" distortion that exists in a steady (periodic) wake or (2) the time-varying distortion or geometry that exists for a nonsteady (nonperiodic) wake.

Thus we need compute only the velocities induced by the wake at the rotor blades, having eliminated the requirement for computing velocities elsewhere in the wake space.

Piziali and DuWaldt [10, 11] have shown that a wake spacing (i.e., of the skewed spiral assumed to correspond to the wake of a rotary wing in forward flight) based on a downward-transport velocity equal to the momentum-theory value of induced inflow yields an azimuthal and spanwise variation of loading in reasonable agreement with experiment. It should be recognized that this particular simplifying assumption (adopted for the SSBL study) is the major feature of the wake model that results in the approach being a practicable one from the standpoint of tolerable computing complexity and cost. Accordingly, no consideration was given towards eliminating this assumption in this study of transient loadings. Note, however, that the existence of a transient wake presents added reasons for the removal of arbitrariness with respect to wake geometry, and accordingly, for the introduction of wake geometry as a dependent variable in the problem. Approximate means for representing the variable geometry in the wake, as exists during the transient interval, are discussed later in this report.

Although the representations of wake vorticity and geometry, as used in the SSBL and TBL models, are mathematically equivalent, there are basic differences in the solution format. In the case of the SSBL calculation, an axis system is placed in the specified (i.e., known) tip-path plane. A set of simultaneous algebraic equations are derived in which the unknown variables to be determined are the bound vorticities that exist on each spanwise blade segment at a finite number of azimuth intervals, this number being taken sufficiently large to describe adequately the azimuthal variation of loading. (This procedure means that the use of 10 spanwise segments and 24 azimuth intervals, for example, requires the determination of 240 unknown circulation strengths.) In the TBL calculation, time-varying loadings cannot be obtained from a simultaneous solution of equations that are based on the periodicity inherent to the steady-state loading process. Rather the bound vorticity existing on the blades at every discrete interval of time (corresponding to an equivalent azimuthal interval) must be determined as a function of the total wake that exists at that specific interval of time Since at any given time interval, the number of unknown circulation strengths that must be determined is the product of the number of spanwise segments and the number of blades, it is seen that, with respect to the requirement for solving a set of simultaneous equations, the TBL calculation is considerably less involved in this regard. On the other hand, whereas the SSBL calculation requires that a solution of a very large set of equations be obtained only once, the mathematical analog of the TBL phenomenon requires that the equation set be solved for each time interval for as many time intervals as are required to define the transient response to a given input of blade-pitch control. This particular feature of the TBL calculation requires that the induced-velocity coefficients of the wake (as defined in Reference 12) be recomputed at each time interval. Note that a SSBL calculation requires

only a single determination of these coefficients.* Accordingly, a TBL calculation procedure must pay a significant penalty in computing time as a consequence of the nonexistence of periodicity in the phenomenon.

The development of the TBL calculation procedure to its present state has required the adoption of the following simplifying assumptions in addition to the above-mentioned (1) neglect of shed vorticity and (2) requirement for specifying wake geometry:

(3) The continuous, spanwise distribution of bound vorticity existing on a real blade, as well as its continuous variation with time, can be satisfactorily defined by using a sufficient number of blade segments and azimuth intervals, over which segment and interval the vorticity is assumed to be constant.

(4) The vortices trailed into the wake are equal to the differences in the strengths of the bound vorticity on adjacent segments of the blade.

(5) The effects of viscous dissipation on the wake-vortex strengths can be neglected.

(6) The angle of attack of a specific blade segment is the "effective" angle of attack computed at the three-quarter chord point.

(7) The circulation trailed into the wake behind a stalled section is the circulation corresponding to the lift produced at the stall angle.

(8) The velocities induced by a rotor wake can be adequately determined by application of the Biot-Savart law.

(9) It is necessary to compute only that component of velocity induced perpendicular to the horizontal line of flight, the lateral and longitudinal components being deemed to be relatively unimportant.

(10) It is permissible to neglect the bound vorticity on the blades in computing the velocities that are induced in the rotating coordinate system since the influence of bound vorticity is negligible at zero forward velocity and remains negligible for low solidities and low advance ratios.

---

*It should be recalled that these coefficients are functions only of wake geometry and rotor position.

(11) The rotor blades are structurally rigid and have only a flapping degree of freedom.

(12) The rotor revolves at a constant angular velocity throughout the transient interval.

(13) The hub of the rotor continues to translate in level, forward flight at constant speed during the short time interval of interest.

Further simplifications that have been introduced into the analysis pertain to the computation of the effective aerodynamic angle of attack and the total aerodynamic force created at a given blade segment. For example, the TBL calculation (in its present form) linearizes the relationships that exist between circulation and induced velocity by assuming that (1) the airflow angle, φ, is small, namely, that

$$\varphi = \tan^{-1} \frac{U_p}{U_T} \simeq \frac{U_p}{U_T},$$

where U_p and U_T are as defined in the List of Symbols, and (2) lift is linearly related to the angle of attack up to an assumed angle of stall, above which the lift coefficient and circulation remain constant. This linearization was incorporated into the SSBL model described in Reference 12 and has been retained here for purposes of simplifying and expediting the solution of the equation set yielding the unknown bound vortices.

DEVELOPMENT OF A SIMPLIFIED WAKE MODEL

As part of the overall effort to develop a method for predicting the nonperiodic air loadings on a helicopter rotor, considerable attention was directed first towards achieving means for simplifying the previously developed wake representation. The motivation was two-fold. First, it was essential that the computation time associated with computing the velocity coefficients of the wake be minimized — particularly in view of the additional computing that is introduced by the step-by-step procedure associated with the TBL process. Second, it appeared desirable to introduce modifications to the original format in order to obtain a more realistic simulation of the rolling-up process that occurs in the wake developed by a rotary wing. To this end, an investigation was made to determine the extent to which the original wake representation, diagrammed schematically in Figure 1, could be simplified and/or modified.

The following wake modifications were examined for their influence on the induced-velocity and loading distributions occurring in forward flight:

(1) Elements of shed vorticity in the wake were neglected at progressively closer points to the blades while retaining a complete mesh of trailing-vortex segments; see Figure 2 (a).

(2) Beyond the shed-vortex truncation point of (1) above, the trailing-vortex segments were concentrated ("rolled up") into a tip and root vortex; see Figure 2 (b). Provision was also made for positioning the root and tip vortices to simulate wake contraction.

(3) Beyond the shed-vortex truncation point of (1) above, the trailing-vortex segments were concentrated into a single tip vortex; see Figure 2 (c).

Calculations were made for the two-bladed HU-1A helicopter flying at 110 knots. Comparisons were made with respect to the azimuthal variations in loading and induced velocity and the harmonic content of these variables up to the tenth harmonic. Typical results (aerodynamic loading plotted versus azimuthal position for a specific spanwise station) are shown in Figure 3 for the following wake configurations:

(1) A complete grid of trailing and shed vorticity.

(2) Shed vorticity truncated at one-quarter revolution behind blade, grid of trailing vorticity retained.

(3) No shed vorticity, grid of trailing vorticity retained.

(4) Shed vorticity truncated at one-quarter revolution behind blade, trailing vorticity rolled up into a root and tip vortex one-quarter revolution behind the blade.

(5) Shed vorticity truncated fifteen degrees behind blade; trailing vorticity "rolled up" into tip vortex only.

Shown also in Figure 3 is representative of similar plots made for other spanwise stations and collectively, these plots demonstrate that the shed vorticity, as represented by the wake model used in the study reported in Reference 12, does not significantly influence the resulting loadings on the blades. The difficulties encountered in adequately representing the shed vortex sheet by discrete vortices located at equally space azimuth intervals behind the blade are reviewed and discussed in Reference 19.

Shown also in Figure 3 are experimental loadings obtained with the HU-1A helicopter [18]. It appears that a wake model consisting only of trailing-vortex elements, trailed as a consequence of a spanwise

variation in bound vorticity, does account for a major portion of the loading phenomena observed in forward flight. Since considerable questions still remained as to the adequacy and necessity of means for representing the shed-vortex sheet, a decision was to drop shed vorticity from the wake model incorporated into the TBL program. Some reservation must be retained, however, as to the adequacy of this simplification when very rapid changes of bound vorticity are produced as a result of (1) very rapid changes in collective pitch, and/or (2) very rapid changes in the induced-velocity field. Admittedly, more calculations are in order to assess the quantitative role of shed vorticity in those flight conditions in which unsteady aerodynamic effects would be accentuated.

During the wake-simplification study, a few calculations were made to investigate the influence of wake contraction on the air loadings produced on a HU-1A rotor at an advance ratio of 0.18. These forward-flight calculations were inconclusive in that no definitive indications could be seen as to whether the simulation of the contraction in the rolled-up wake yields improved correlation with experiment. Subsequent calculations made for hovering flight, on the other hand, produced just the opposite result, namely, that simulation of wake contraction is a feature of a wake model that is essential to the prediction of the aerodynamic loading in hover. A few remarks relative to this point are in order.

Since the objective of the SSBL research program was the development of means for predicting the highly variable loadings produced in forward flight, no attention had been directed to hovering flight. Thus, no knowledge was available as to the ability of the SSBL wake model to predict total loads and load distributions of reasonable accuracy for a hovering rotor. In this investigation the response of a hovering rotor to rapid changes of collective pitch, was however, a matter of interest. It was, therefore, necessary to obtain a steady-state loading in hover for purposes of representing the initial condition that prevails prior to the initiation of the transient input. Calculations showed that a wake model without any contraction assumed for the rolled-up portion yielded both a total load and spanwise distribution of loading that were in poor agreement with the results measured on an H-34 helicopter [20]. Figure 4 shows the nature of this discrepancy and presents also the considerable improvement in the calculated result when the rolled-up tip vortex is assumed to be located at $r/R = 0.825$ and the rolled-up root vortex is assumed to be located at $r/R = 0.425$.

It is concluded that realistic predictions of loading during hover can be obtained only if the wake geometry is suitably specified to approximate the actual contraction of the wake. Further, the limited wake studies conducted in this investigation indicate that the variable loadings produced for forward flight in the vicinity of $\mu = 0.18$ are caused by geometrical features of the wake that can be described satisfactorily

irrespective of small errors in the estimates of (1) the degree of wake contraction and (2) the value of the vertical-transport velocity. The spanwise load distributions produced during hovering, on the other hand, are sensitive functions of geometry of the wake — in particular, the pitch of the vortex spiral and the diameter of the spiral formed by the rolled-up tip vortex.

THE COMPUTATIONAL MODEL

A mathematical analog of an articulated rotor, with rigid blades flapping in the induced-velocity field created by the vortical wake of the rotor, consists of several major parts. These are as follows:

(1) The equations that yield the geometry of the wake, i.e., the spatial location and orientation of elements of vorticity in the wake relative to the blades of the rotor at each and every instant of time. (Wake geometry is determined by the specified flight condition and rotor configuration, the motions of the rotor blades, and the vertical-transport velocity. This latter variable is specified as a constant for calculating steady-state loadings and as a function of time when computing transient loadings.)

(2) The application of the Biot-Savart law to compute the induced-velocity coefficients corresponding to the wake geometry existing at a given instant of time. (These induced-velocity coefficients represent the velocity induced by a given segment of wake at a specific location in the rotor disc per unit strength of vorticity in the wake element.)

(3) The assignment of circulation strengths to each element of wake at each instant of time as a function of all the vorticity that has been trailed at earlier instants. These vorticities are functions of the bound vorticities that existed at earlier times.

(4) The summing of induced-velocity contributions from all elements of the wake except for the elements of unknown strength immediately adjacent to the blades.

(5) The equations defining the angle of attack of the blade segments as a function of the kinematics of the rotor and the velocities induced by all of the vorticity in the wake, except the vorticity being trailed at the given instant of time.

(6) The set of simultaneous equations that relate at the given instant of time the unknown bound circulations (and

likewise the trailing vorticities adjacent to the blades) to those values of circulation corresponding to the angles of attack determined in (5) above.

(7) The equations defining aerodynamic loading, moment about the flapping hinge, and angular acceleration of the blade about the flapping hinge.

(8) A numerical integration procedure to obtain the angular velocity and displacement of the blade about the flapping hinge.

Figure 5 is a schematic of the above-outlined mathematical analog. (The details of the complete mathematical model are presented in Appendix 1.) It is sufficient to note here that the computations indicated in Figure 5 are carried out for as many time intervals as may be necessary to (1) establish a periodic loading and wake and (2) determine a complete time history of the transient response to a specified change in collective pitch, that is, until the loading and wake again become periodic with time.

The calculations diagrammed in Figure 5 require that an axis system be defined for describing both the flapping response of the rotor and the geometry of the wake. Figure 6 shows the x-y-z axis system adopted for this purpose. Note that the origin is placed at the hub of an articulated (flapping) rotor, with the x axis directed rearward, parallel to the horizontal direction of flight. It should be recalled that the analysis is restricted to level-flight operations or to the situation that prevails when the rotor hub is held fixed in a wind tunnel. Figure 6 shows that the rotor shaft has been assumed to be tilted only in the x-z plane. Thus we ignore any lateral tilt of the rotor shaft, since this tilt angle is usually small during trimmed, level flight. A conventional shaft axis system is used to describe the flapping and feathering of the blades and the motions and displacements of the blades (as seen in the shaft axis system) are transformed to equivalent quantities in the x-y-z system. Only the z-axis component of the total induced-velocity vector is included in the analytical model, as was indicated earlier. In accordance with the adopted axis system, velocities induced in the negative z-direction are designated as negative quantities.

COMPARISON OF THEORY AND EXPERIMENT

STEADY-STATE LOADINGS

The measured air loads used to test the adequacy of the TBL computational model for predicting periodic loadings in steady flight were obtained from two sources: full-scale flight tests of the H-34 helicopter [21] and wind-tunnel tests of a full-scale H-34 rotor [22]. The first set of data is a portion of the data originally used to evaluate the adequacy of the SSBL calculation procedure [12]. Data obtained at one specific flight condition ($\mu = 0.18$; $V = 118$ fps) are employed herein to examine the extent to which the current SSBL and the TBL computational procedures yield results in agreement with each other and with experiment. Although it is patently true that the successful prediction of transient loadings requires, a priori, a model that correctly predicts periodic loadings for steady flight, it was felt that steady-state comparisons are also mandatory to demonstrate that the TBL procedure yields periodic loadings for steady forward flight equivalent to that calculated by another computational method.

Figure 7 presents the aerodynamic loadings at seven spanwise stations as a function of azimuth, as obtained by measurement and by computation with the SSBL and TBL programs. The differences between the results produced by the two computational procedures can be attributed to the differences that exist between first-harmonic flapping, that is, the tip-path-plane orientation. It should be noted that the SSBL calculation procedure described in Reference 12 requires that the tip-path-plane orientation be known and specified as an input to the program. In the TBL calculation, however, the blades are free to flap and the steady-state orientation of the tip-path plane is a computed quantity. Small differences between specified and computed first-harmonic flapping of the blade result in significant differences in the first-harmonic variation of angle of attack. These differences in computed angle of attack caused by small discrepancies in first-harmonic flapping are responsible for the discrepancies in computed loadings seen in Figure 7. Notwithstanding this failure of the SSBL and TBL calculation procedures to agree on first-harmonic components of the air loading, a comparison of the measured and computed loadings in Figure 7 shows that theory predicts the higher frequency variations in measured load reasonably well.

Figure 8, a plot of induced velocities versus azimuth for seven different spanwise positions, demonstrates that the SSBL and TBL calculation procedures yield, for all practical purposes, the same induced-velocities in the plane of the rotor disc. This figure is included for purposes of demonstrating that the differences between the calculated loadings presented in Figure 7 cannot be attributed to a lack of equivalence in the induced velocity field yielded by two different calculation procedures.

The question as to why the TBL computation yields a tip-path-plane angle of 4.2 degrees in contrast to the angle of 3.0 degrees specified as the input to the SSBL computation cannot be answered in a precise manner. There are many approximations and simplifications (as well as inaccuracies of measurement) that lead to small differences in load and load distribution which, in the aggregate, can cause differences in blade motion of the magnitude obtained. It should be emphasized that while accurate prediction of blade motions is necessary to obtain accurate predictions of blade loadings, it is by no means sufficient.

Figure 9 is a comparison of calculated periodic air loadings (i.e., in steady forward flight with data obtained in full-scale wind-tunnel tests [22]. The loadings plotted in this figure correspond to the initial steady state achieved in Run 1 (see table on the following page for listing of test conditions - Runs 1, 2, and 3) prior to the initiation of a collective-pitch change. In general, the agreement between theory and wind-tunnel test appears to be as good or better than that achieved with full-scale flight data (see Figure 7). Since the agreement that is obtained is, in part, a function of the advance ratio and total force, it is not possible to draw any firm conclusions as to whether the improved agreement reflects more accurate input data or is the result of the air loadings being less sensitive to the wake for this particular flight condition. It should be noted, however, that the comparisons made in Figure 7 involve calculations in which no wake contraction was introduced whereas the tip and root vortices were assumed to roll up 45 degrees of azimuth behind the blade at the 0.90 and 0.375 radial stations, respectively, in the calculations plotted in Figure 9. No calculations have been made without wake contraction being assumed for the test conditions corresponding to the results presented in Figure 9.

RESPONSE TO CHANGE IN COLLECTIVE PITCH

The measured air loads used to test the adequacy of the TBL computational model for predicting the transient response to a change in collective pitch were obtained in wind-tunnel tests, as indicated above. Data were obtained at two "flight" conditions. For the first condition, one transient response was produced by a rather slow increase in collective pitch. In the second condition, two transients were produced, one in response to a more rapid increase in collective pitch, a second in response to a rapid decrease. Data pertaining to the wind-tunnel test conditions are tabulated in the table.*

* Originally a more exhaustive test program was planned, but instrumentation difficulties forced the curtailment of the transient-response tests.

In order to facilitate a comparison between theory and experiment, it was necessary first to reduce the test data for purposes of determining the cyclic-pitch settings and time history of collective pitch. Since blade pitch was measured on blades separated by 180 degrees of azimuth, collective pitch could be resolved by summing the output of these pitch transducers. Cyclic pitch was then determined by subtracting collective from the pitch of the instrumented blade.

TABLE I
WIND TUNNEL TEST CONDITIONS

	RUN 1	RUN 2	RUN 3
AVERAGE TEST VELOCITY, FT./SEC.	131.0	186.0	186.5
ROTOR ANGULAR VELOCITY, RAD./SEC.	23.2	23.2	23.2
ADVANCE RATIO	0.202	0.286	0.287
SHAFT ANGLE OF ATTACK, DEG.	10	5	5
AVERAGE AIR DENSITY, SLUGS/CU.FT.	0.0022[illegible]	0.002276	0.002272
INITIAL TOTAL LIFT, LBS.	8710	8945	8715
FINAL TOTAL LIFT, LBS.	12182	*	2037
TOTAL COLLECTIVE-PITCH INCREMENT, DEG.	1.775	1.607	-2.663
RATE OF CHANGE OF COLLECTIVE PITCH (NOMINAL VALUE) DEG./SEC	6.55	12.95	-47.2

*NO WIND-TUNNEL BALANCE READING BECAUSE OF EXCESSIVE VIBRATION.

The above procedure worked very well with respect to determining the relative variation in collective-pitch settings, but the absolute values of collective pitch, as indicated by the measured traces and the supplied calibration data, were so small that negative thrust would result in a subsequent computation. It proved expedient to resort to the charts presented in Reference 23 to determine appropriate settings of collective pitch and to utilize further that portion of the TBL program which operates with a specified inflow to check these settings for suitable accuracy. Subsequent to this step, as made necessary by the invalid experimental data, three complete transient responses were computed for comparison with actual measurement.

Figures 10, 11, and 12 present comparisons of measure and predicted transient air loadings for seven span positions for test runs 1, 2, and

3, respectively.* Shown also are predicted and measured flapping, the time history of collective pitch (as measured and as used for the input to the calculation), and the assumed variation in the mean induced velocity, $\bar{w}$, governing the spacing of the wake during the steady and transient interval. The assumed timewise variation in $\bar{w}$ was based on the results of hovering calculations that are discussed in the following section of the report. As a result of this hovering study, there is reason to believe that the computed air loadings would not be modified significantly on assuming a different time variation in $\bar{w}$. Instead, it appears that wake distortion arising from self-induced effects, in all likelihood, contributes errors in the description of wake geometry that are considerably more significant than the errors that result from the very approximate means used to simulate the time-varying spacing of the wake spiral during the transient interval.

Figures 10, 11, and 12 show that the TBL model developed in this study simulates in remarkably good fashion the overall behavior of a rotary wing subjected to a change in collective pitch. Although the computations do not produce precise agreement with the measured time histories of air loadings, there are many areas of qualitative and quantitative agreement. It is seen that certain portions of the high-frequency content in the loadings are predicted by theory remarkably well. Note should be taken of the agreement between theory and experiment as reflected by the different patterns of loading that occur at the various radial positions on the blade. Note also the agreement achieved between measured and predicted flapping.

These comparisons of measured and calculated responses would appear to indicate that continued refinements of the analysis with respect to (1) the aerodynamics, (2) improvements in the description of wake geometry, and (3) expanded modeling of the rotor structure will lead to an even better prediction capability. It is concluded that the wake model, in its present form, together with a model of the kinematics and dynamics of a simple articulated, rigid-blade rotor simulates the essential components of the TBL phenomenon resulting from typical changes in collective pitch. Admittedly, additional data are needed at lower and higher advance ratios in order to further confirm or qualify this conclusion.

---

* It should be noted that a $r/R = 0.95$, the calculated response corresponds to $r/R = 0.96$ as a result of a requirement (to be discussed later) to compute the loadings at eight spanwise segments.

A comment is in order with respect to the total thrusts that are predicted by a nonuniform-inflow calculation. As was mentioned above, the collective pitch was adjusted until a uniform-inflow calculation yielded a calculated total thrust equal to the total thrust measured in the wind tunnel. In actual practice, allowance was made for the fact that the integration (trapezoidal) of load along the span yields calculated total blade loads that are less than the true load. For example, the use of eight spanwise segments in the calculation results in a three-percent reduction from the load yielded by the use of nine segments. Accordingly, the initial collective pitch was set in Run 1 to produce an average load of 8450 pounds, with the uniform-inflow computation indicating a four-per-revolution oscillatory component of approximately 60 pounds. It was found that the steady total load, as yielded by a nonuniform-inflow calculation, is approximately 8150 pounds and has a four-per-revolution oscillatory component of approximately 755 pounds. Two observations can be made:

(1) The average total lift resulting from a nonuniform-inflow calculation is less than that yielded by a uniform-inflow calculation.

(2) A significant level of oscillatory total shear at the rotor hub is predicted by a nonuniform-inflow calculation whereas very little oscillatory component is predicted by a uniform-inflow calculation.

The above comparisons have significance with respect to calculations of rotor performance and transmitted shears.

Note that Figures 10, 11, and 12 do not readily indicate whether discrepancies, if any, exist between the calculated and measured mean loadings. The calculations, as performed, yielded mean total thrust approximately 4 percent less than the initial and final mean steady-state thrusts measured for all three runs with one exception — the calculated average thrust for the final steady state achieved in run 3 is approximately 2600 pounds (i.e., about 30 percent greater than the measured value). These discrepancies in the mean thrust levels obviously do not detract from the basic validity of Figures 10, 11, and 12 for demonstrating the ability of the TBL model to predict variations in air loading, either with respect to spanwise position on the blade or azimuthal location in the rotor disc.

ADDITIONAL NUMERICAL INVESTIGATIONS

The development of a method for computing the transient air loadings on rotary wings has necessarily resulted in several additional numerical studies. The results obtained in these studies have yielded additional insight on (1) the nature of the blade-loading phenomenon and (2) the capabilities and shortcomings of the developed analytical procedure. Several of these results will be discussed in this section of the report.

Consideration of the blade-load prediction task shows that there are several sources of error. One source is the erroneous contribution to the angle of attack of a blade segment that results from geometric angles of pitch and blade pitching/plunging velocities that are not in accord with actuality as a result of assuming that the blades are rigid or as a result of insufficient rigor in modeling either the elastic structure of the blade or the kinematics of the hub. A second source is the erroneous induced-velocity field that results from our inability to model the wake, both its geometry and strength, with sufficient exactitude. With respect to the first source of error, studies are underway in several organizations (including CAL) to determine the extent to which predictions of blade loading can be upgraded by appropriate modeling of the elastic properties of rotor blades [19]. With respect to the second source of error, the extent to which improved modeling of the geometry of the wake will yield significant gains in load-prediction accuracies is a matter of much concern. On the other hand, there is considerable motivation (as was pointed out earlier) for simplifying the model of the wake in order to reduce the program size and the amount of computing time that is currently required. Further, questions of the adequacy of wake models become considerably more involved when transient (nonperiodic) loadings are of interest rather than the periodic loadings produced in steady, forward flight. Accordingly, consideration is given, in this section of the report, to certain aspects of wake modeling, both for the steady-state and transient flight regimes.

The contribution of the wake in causing blade-load variations of high harmonic order is graphically demonstrated in Figure 13. Computed total lifts on an H-34 rotor blade are shown plotted versus azimuth. The dashed curve is the total load that is computed when the inflow is assumed to be constant. The solid curve is the result that is obtained when the inflow is a function of the velocities induced by the vorticity in the wake.

Although the vorticity distribution in the wake corresponding to the lift on the blade represented by the solid line is significantly different from that associated with the lift on the blade represented by the dashed line, we find that the induced-velocity distributions produced are very similar. Figure 14 shows the spanwise variation of induced velocity on four blades if the computation is made at an instant of time at which all the vortex elements in the wake have strengths corresponding to the load variation

represented by the dashed line in Figure 13. Figure 14 also shows the induced velocity versus span that results from a wake having the vortex strengths associated with the solid line in Figure 13. It appears reasonable to conclude (at least on a tentative basis) that the velocities induced in the plane of the rotor disc are more sensitive functions of wake geometry than of the vortex strengths. These calculations appear to lend support to the hypothesis that a wake having a constant strength corresponding to the mean total load on a rotor would produce a good approximation of the velocity field that is induced in the plane of the rotor disc. Additional numerical studies are required to confirm this hypothesis fully and to establish the degree of approximation involved.

The problem of modeling rotor-wake geometry during the transient interval that is associated with a change in collective pitch has been mentioned previously. Note that it is theoretically possible to account for both the steady-state and transient distortion in a wake by computing the velocities that are induced everywhere in the wake space. However, the realities of required computing time and cost rule out this approach to the problem. Fortunately, reasonably good predictions can be made of the periodic loadings in steady, forward flight when the self-induced distortions in the steady wake are ignored [12]. On the other hand, it is not possible to ignore, a priori, the time-varying geometry of the transient wake since the assumption made with regard to a uniform and constant velocity transporting wake elements in the downward direction may no longer be admissible. A short numerical investigation of this point was made.

Since the mean velocity induced by the wake is greatest in hovering flight, it was hypothesized that the transient loadings resulting from a collective-pitch change introduced during hover would be most sensitive to transient spacing in the wake spiral. Accordingly, a series of calculations were made for a H-34 rotor at zero flight velocity in order to investigate the importance of transient wake effects. Responses to both positive and negative changes in collective pitch were obtained.

Figure 15 is a time history of loading, total thrust on rotor, total thrust on blade, flap angle, circulation, and induced velocities as caused by a change in collective pitch of approximately four degrees. The solid curves were obtained for a wake whose spacing remains fixed at its initial steady-state value. The dashed curves were obtained when the mean value of induced velocity, transporting the wake, was assumed to vary with time as shown.* Note that the collective-pitch ramp is

---

* As a result of an error in the computation of the aerodynamic moment about the flapping hinge, all hovering computations predict a coning angle that is much too large. Conclusions drawn with respect to loading and the effects of transient wake geometry are still valid, however.

completed in a time interval required for the rotor to rotate through 60 degrees of azimuth. The blade-pitch rates that exist during the input interval are quite large and the observed discontinuities in the loading time histories, etc., result from the effective angles of attack caused by the high rate of blade pitch that exists over the input interval. We observe that the total thrust on the rotor reaches its peak value approximately three-quarters of a revolution after initiation of the collective-pitch ramp. It should be noted that the overall behavior of the rotor, i.e., the predicted total thrust and flap response, is similar to the experimental results obtained previously by Carpenter and Fridovich [13].

Of particular interest to this investigation are the changes in loading and load distribution that result from a transient input and subsequent variations in the geometry of the wake. Note that the loadings do not reach their peak values simultaneously; specifically, the center-span blade segments reach their peak loading prior to segments near the tip of the blade.* This result is caused by differences in the timewise variation in induced velocity at the various radial positions. The time histories show that the induced velocities change immediately following the initiation of the input at those stations located at the tip and root ends of the blade. At the median stations, there is a time delay before any significant change is exhibited by the induced velocity.

When the mean induced velocity, $\bar{w}$, varies as shown by the dashed line**, we find, first, that the final steady state is attained at an earlier time since the increased wake spacing decreases the influence of the "older" wake elements. Second, we observe, as expected, that the final total thrust on the rotor is increased. Third, the time histories of blade loading are similar to those computed previously, with the exception that at r/R = 0.55, 0.65, and 0.75 we observe (1) an "undershoot" as well as an "overshoot" in loading, and (2) greater percentage differences in the final steady-state loading. Fourth, these observed changes in load distribution along the span are accounted for by the different induced-velocity field that results when the wake spacing is assumed to increase in the manner shown. It is seen that the increased wake spacing causes a relatively small increase in the velocities induced near the tip of the blade, whereas at r/R = 0.55, 0.65, and 0.75 a significant reduction occurs in the velocities induced by the wake. In general, it may be stated that it is primarily the mid-span locations on the blade that exhibit a change in steady-state loading due to a specified change in wake geometry and these locations likewise exhibit the largest transient effects that depend on the manner in which the mean value of the induced velocity is assumed to change.

---

* The loading at the 25-percent span position remains constant since this segment of the blade is stalled.

** The final value of $\bar{w}$ is based on a prior estimate of the final total thrust.

The response of a hovering rotor to a reduction in collective pitch is presented in Figure 16. The mean induced velocity, $\overline{w}$, was assumed to vary in the manner plotted. This assumption was based on a prior estimate of the final value of total thrust to be achieved with the reduced collective pitch, with the timewise variation being based on the induced-velocity responses computed for the increase in collective pitch.

Another aspect of the wake model, deserving of consideration, is the assumption that the trailing vorticity streams rearward (with the local velocity vector) from the bound vortex located at the one-quarter chord. This assumption has created a computational limitation in that an upper limit exists on the advance ratios that can be treated, this limit being a function of the spanwidths specified for the blade segments used in the computation. The limitation arises from the "lumping" process used to represent the trailing vortex sheet. Specifically, the representation of the trailing wake by discrete vortices implied selection of control points for computing induced velocities that are midway between trailing vortex filaments. Under the present assumption of vortices trailing free from the one-quarter chord, it is possible for the three-quarter chord point on the blade to fall outside the horse shoe vortex associated with that particular blade segment. This resultant geometry can occur for a combination of very narrow segments (usually taken at the blade tip) and high advance ratios. The computation will fail whenever this situation occurs since the trailing vortices do not act to restrain the bound circulation at this segment, but rather become a destabilizing influence in the solution for the unknown bound circulation strengths.

Previously, Queijo has shown [24] that a better representation of spanwise-flow effects on a sideslipping wing consists of trailing vortex elements that remain fixed in the wing (parallel to the chord-wise direction) until they stream free at the trailing edge, a geometry originally proposed by Weissinger [25]. Experience with the TBL computational procedure indicates that modification of the TBL model to incorporate the trailing-vortex geometry first proposed by Weissinger [25] will have a twofold benefit. First, the existing restriction on advance ratio and segment widths will be removed. Second, the approximation introduced by dividing the blade into a finite number of spanwise segments will be improved, since the problem associated with calculating induced velocity at points exceedingly close to a vortex element will be eliminated.

A final comment with respect to the adequacy of the adopted wake model bears on the question of the circulation strengths assigned to the rolled-up root and tip vortex. Calculations made during the wake-simplification study, for one specific rotor and flight configuration, indicated that the maximum circulation on the blade did not move radially to any significant extent. Further, the circulation distribution

tended to be relatively flat near the peak. Accordingly, it appeared reasonable to assign the circulation strength computed at the specific radial station bracketing the average location for peak gamma, Γ , to the rolled-up root and tip vortices. This procedure obviated the need for program logic to seek the maximum value of Γ along the blade span and thereby simplified the computational procedure. Calculations made for the purpose of comparing theory with data obtained in the NASA-Ames Tunnel have shown, however, that "flight" conditions can exist wherein the location of peak Γ moves almost from root to tip in an erratic fashion during one rotor revolution. It appears that the scheme adopted herein for assigning circulation strengths to the rolled-up wake is not always a good approximation. Thus, an error of uncertain magnitude has been introduced into the transient-response computations performed during this investigation. Future modeling of rotor-wake systems should make due allowance for the fact that the spanwise location of maximum circulation is not as stationary as was assumed in this study.

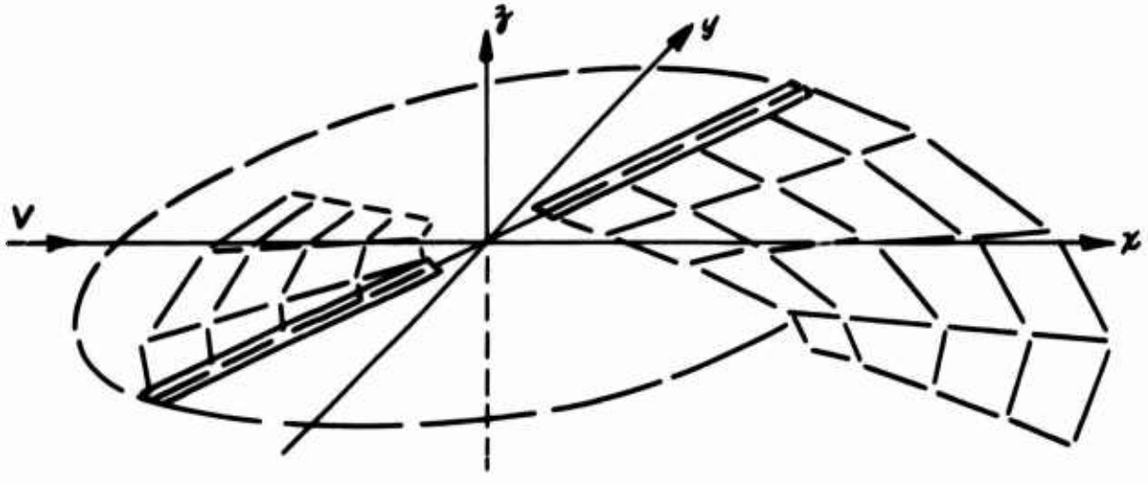

Figure 1. PICTORIAL EXAMPLE OF THE INITIAL PORTION OF THE WAKE OF A TWO-BLADE ROTOR DIVIDED INTO FOUR RADIAL SEGMENTS.

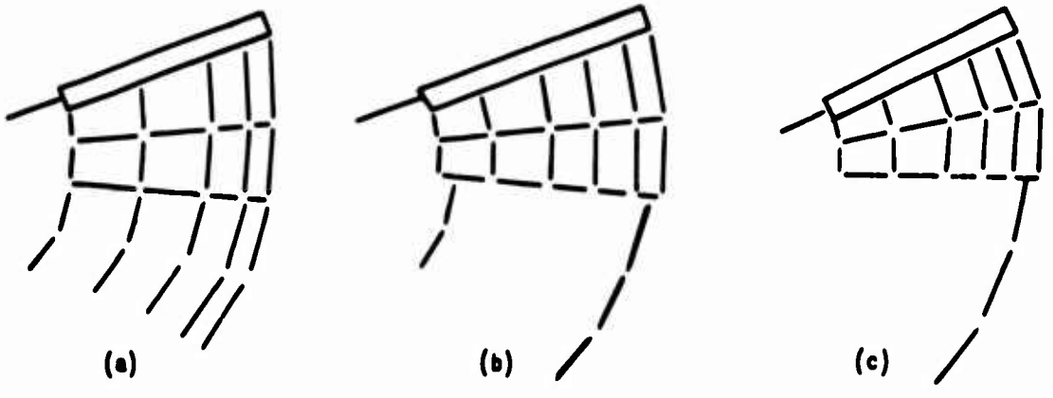

Figure 2. WAKE MODELS EXAMINED IN A WAKE-SIMPLIFICATION STUDY.

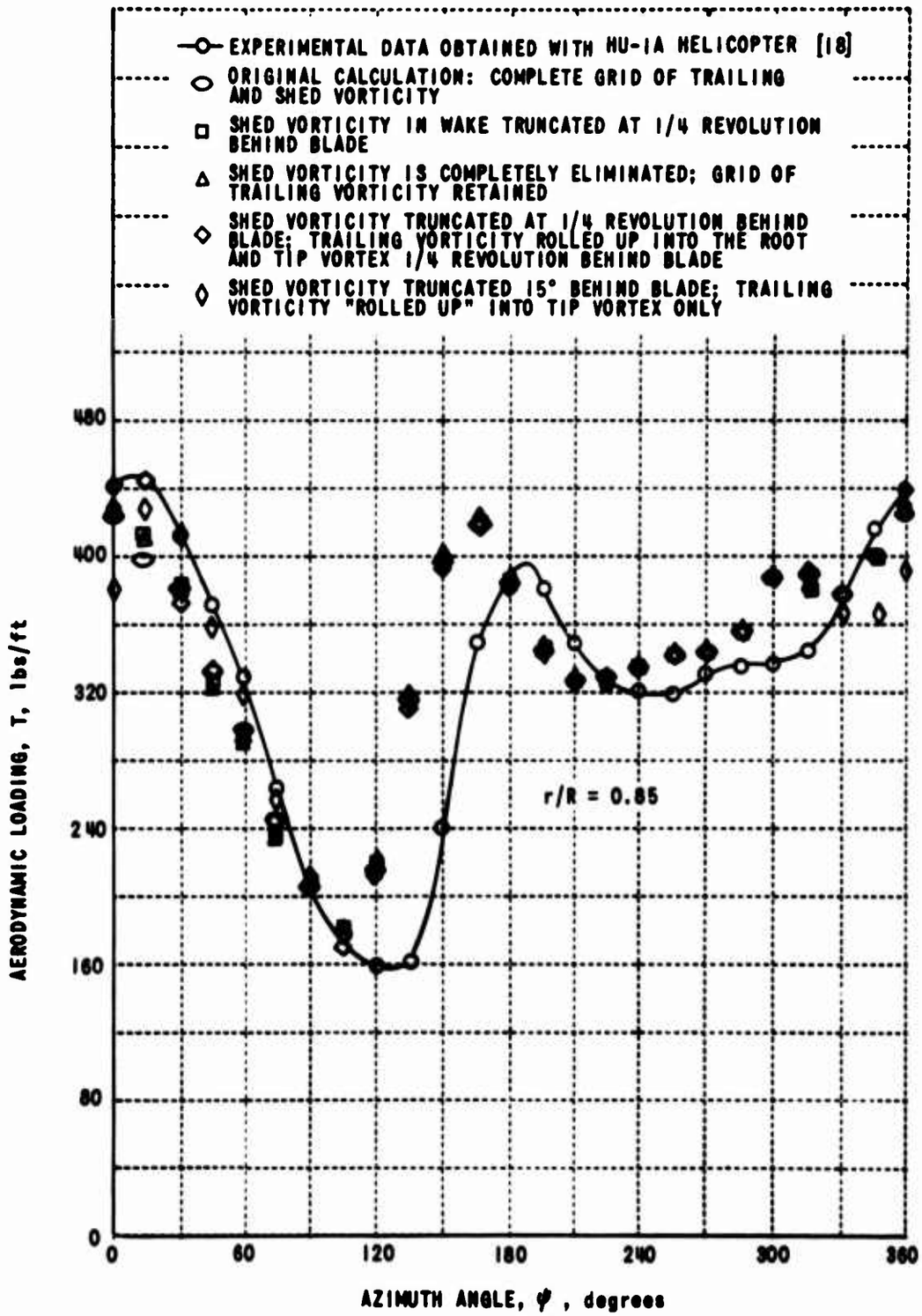

Figure 3. INFLUENCE OF WAKE REPRESENTATION ON COMPUTED AERODYNAMIC LOADING vs. AZIMUTH ANGLE.

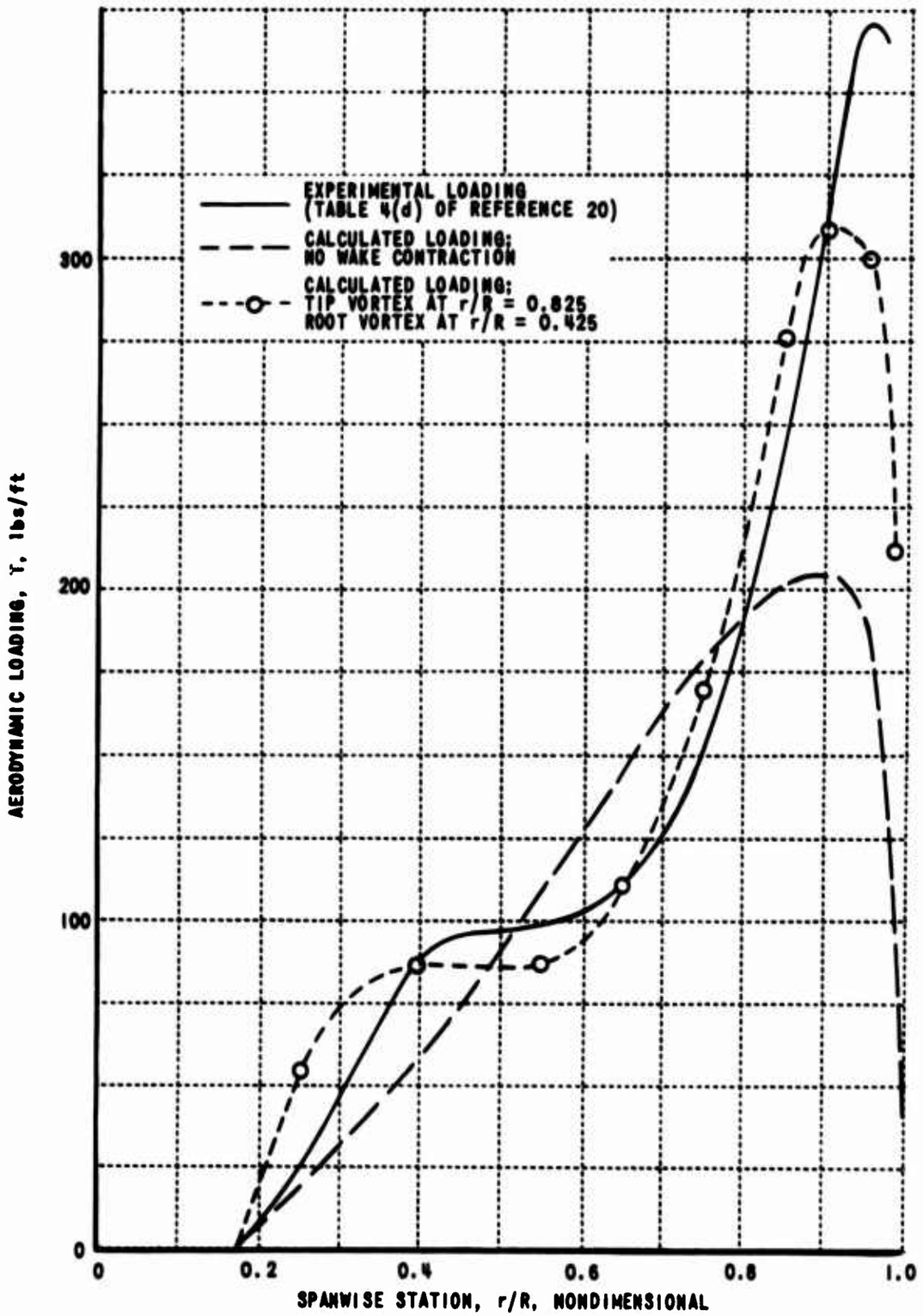

Figure 4. COMPARISON OF CALCULATED AND MEASURED LOADINGS IN HOVERING FLIGHT.

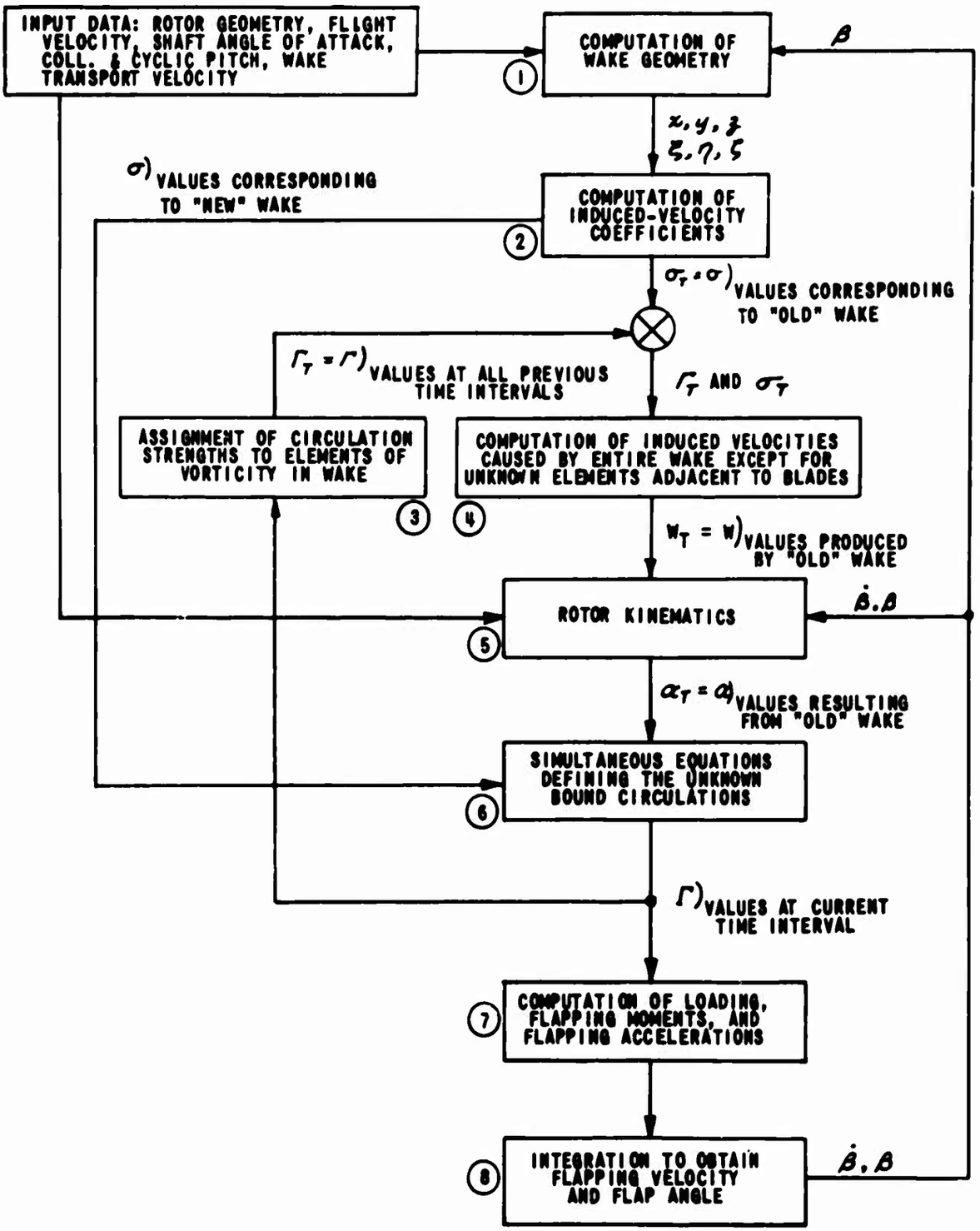

Figure 5. SCHEMATIC DIAGRAM OF TBL MODEL.

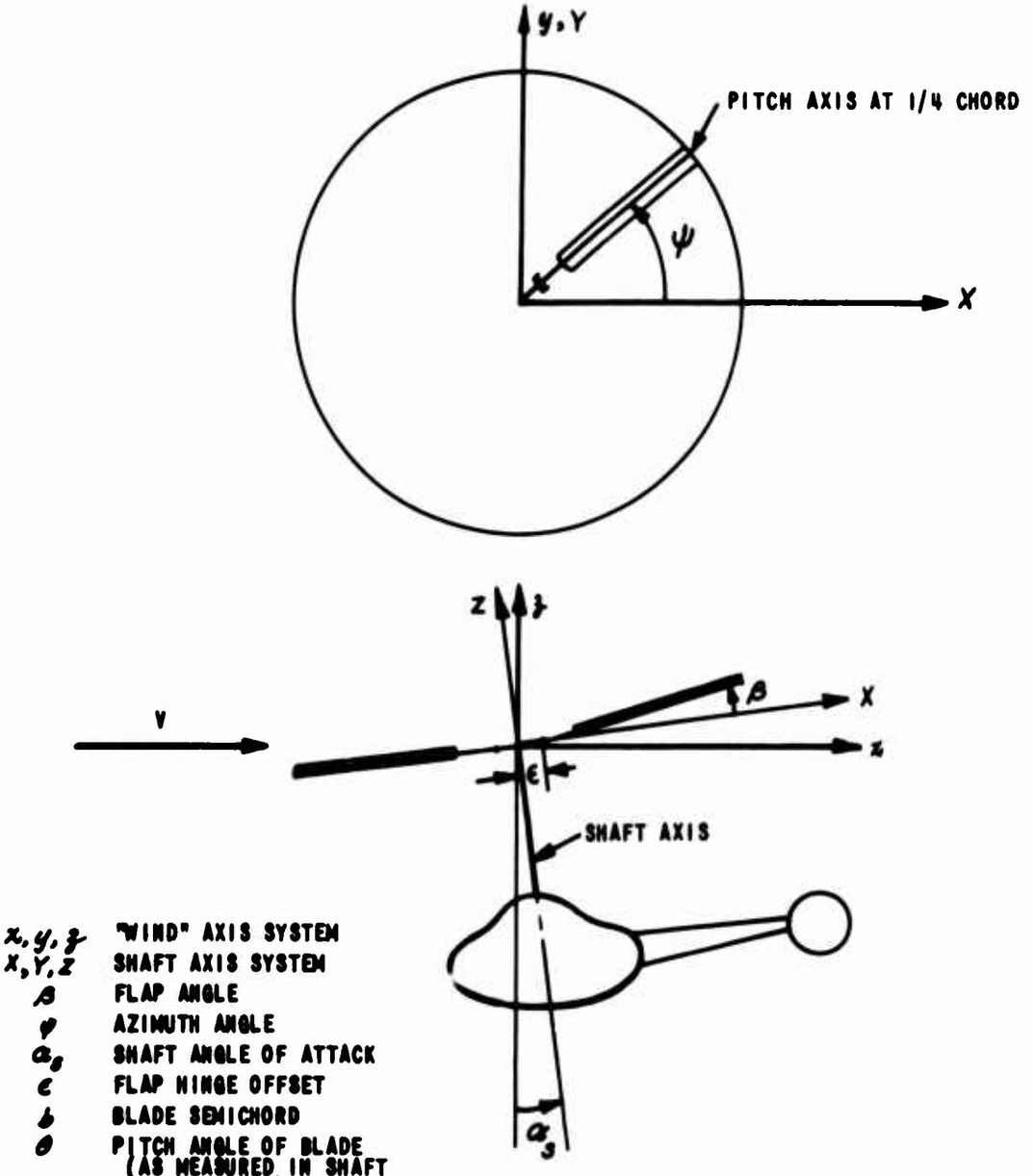

Figure 6. AXIS SYSTEM USED IN TBL ANALYSIS.

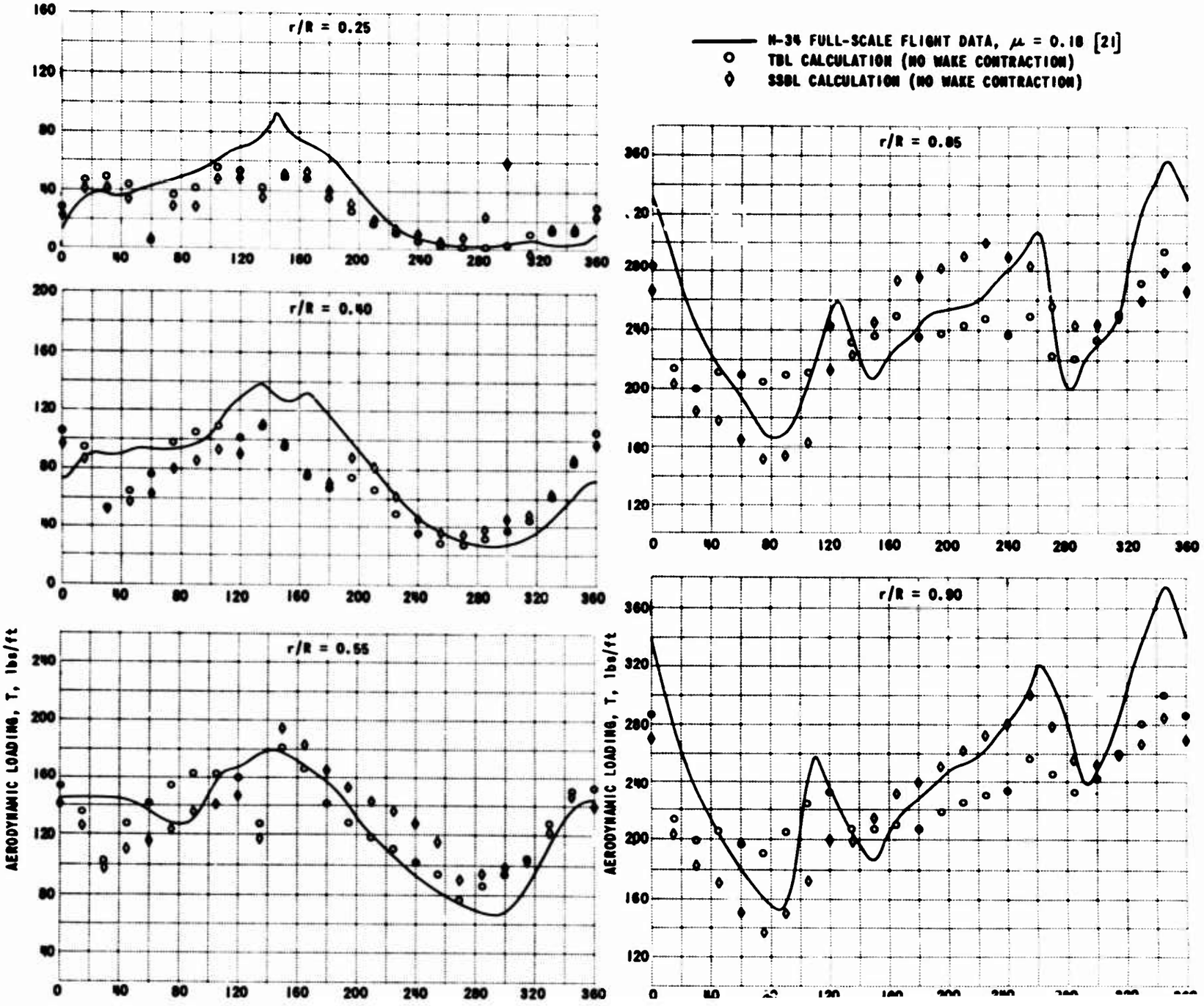
N-34 FULL-SCALE FLIGHT DATA, μ = 0.18 [21]
TBL CALCULATION (NO WAKE CONTRACTION)
SSBL CALCULATION (NO WAKE CONTRACTION)
r/R = 0.25
r/R = 0.40
r/R = 0.55
r/R = 0.85
r/R = 0.90
AERODYNAMIC LOADING, T, lbs/ft

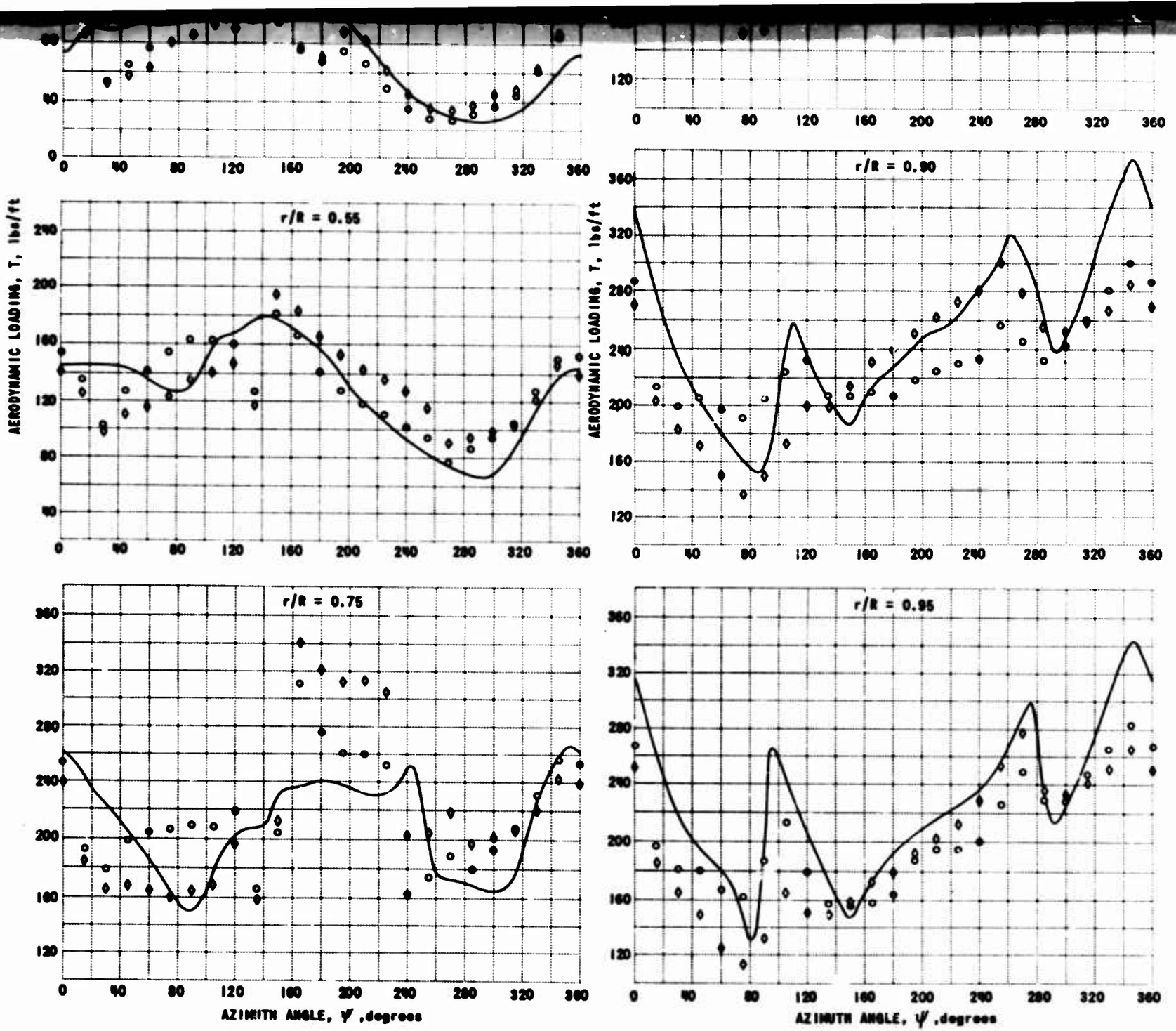

Figure 7. STEADY-STATE AERODYNAMIC LOADINGS vs. AZIMUTH ANGLE; H-34 ROTOR, μ = 0.18.

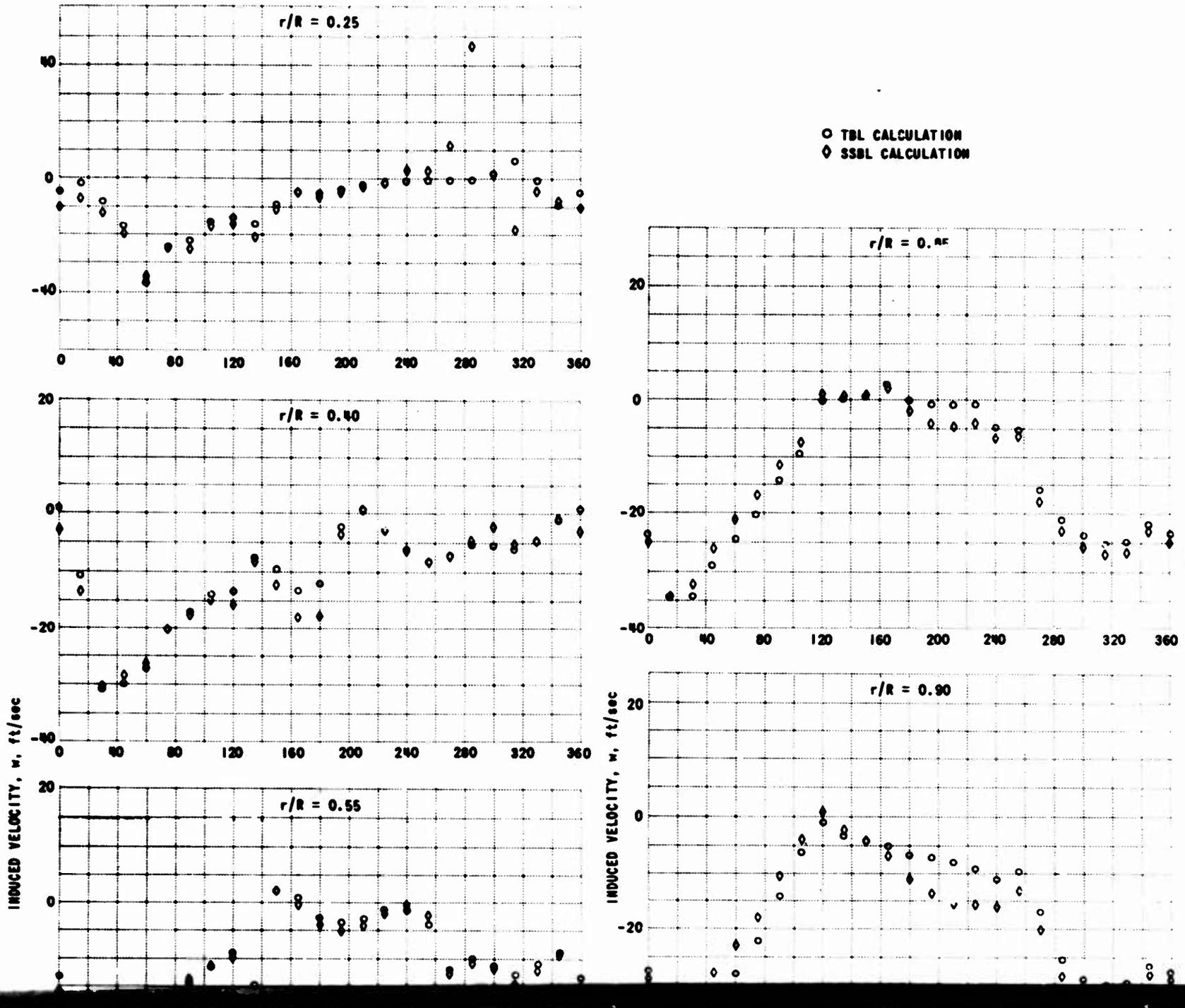
r/R = 0.25
r/R = 0.40
r/R = 0.55
r/R = 0.85
r/R = 0.90
O TBL CALCULATION
◊ SSBL CALCULATION
INDUCED VELOCITY, w, ft/sec
0
40
80
120
160
200
240
280
320
360
20
0
-20
-40

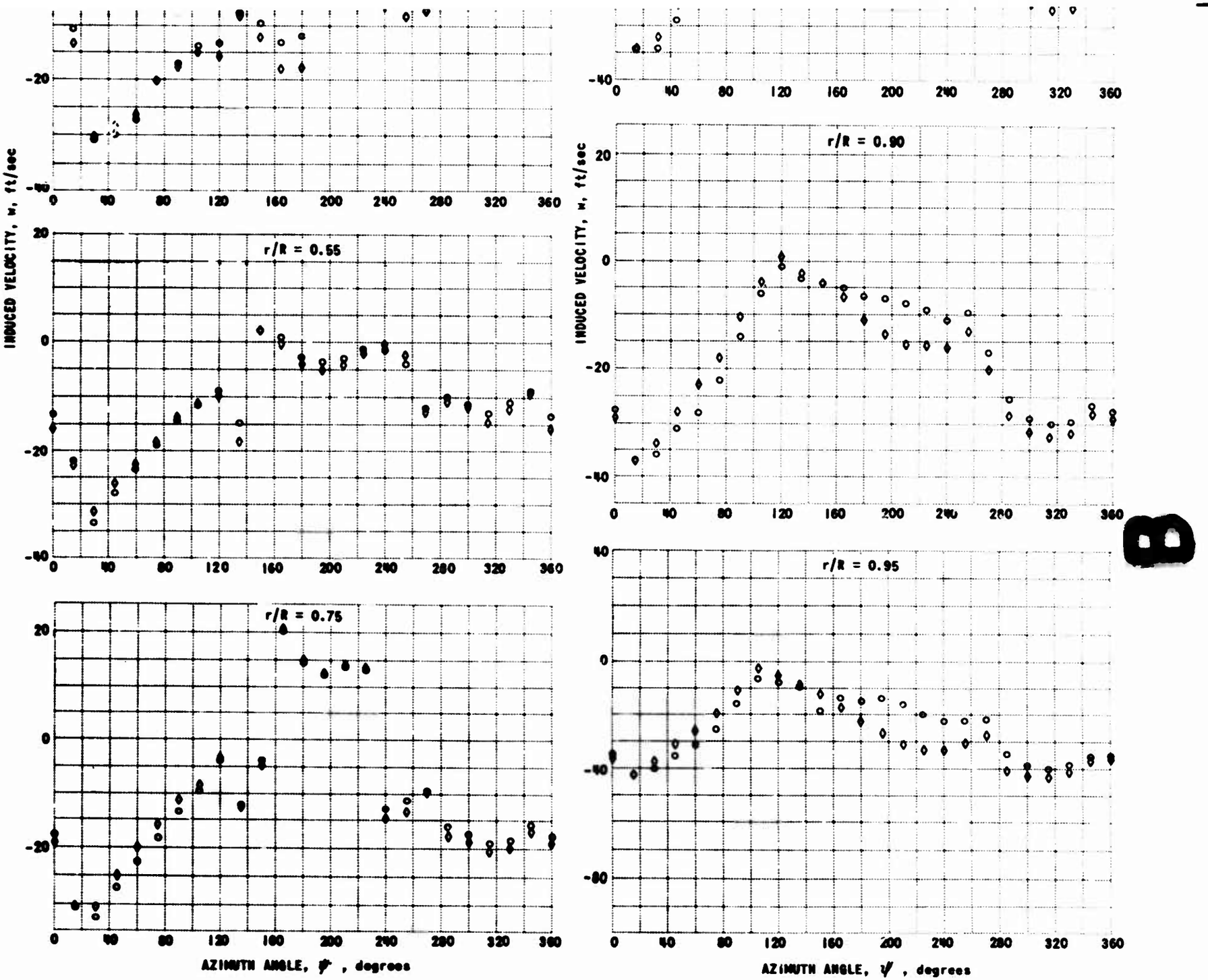

Figure 8. COMPARISON OF INDUCED-VELOCITY DISTRIBUTIONS YIELDED BY SSBL AND TBL CALCULATIONS.

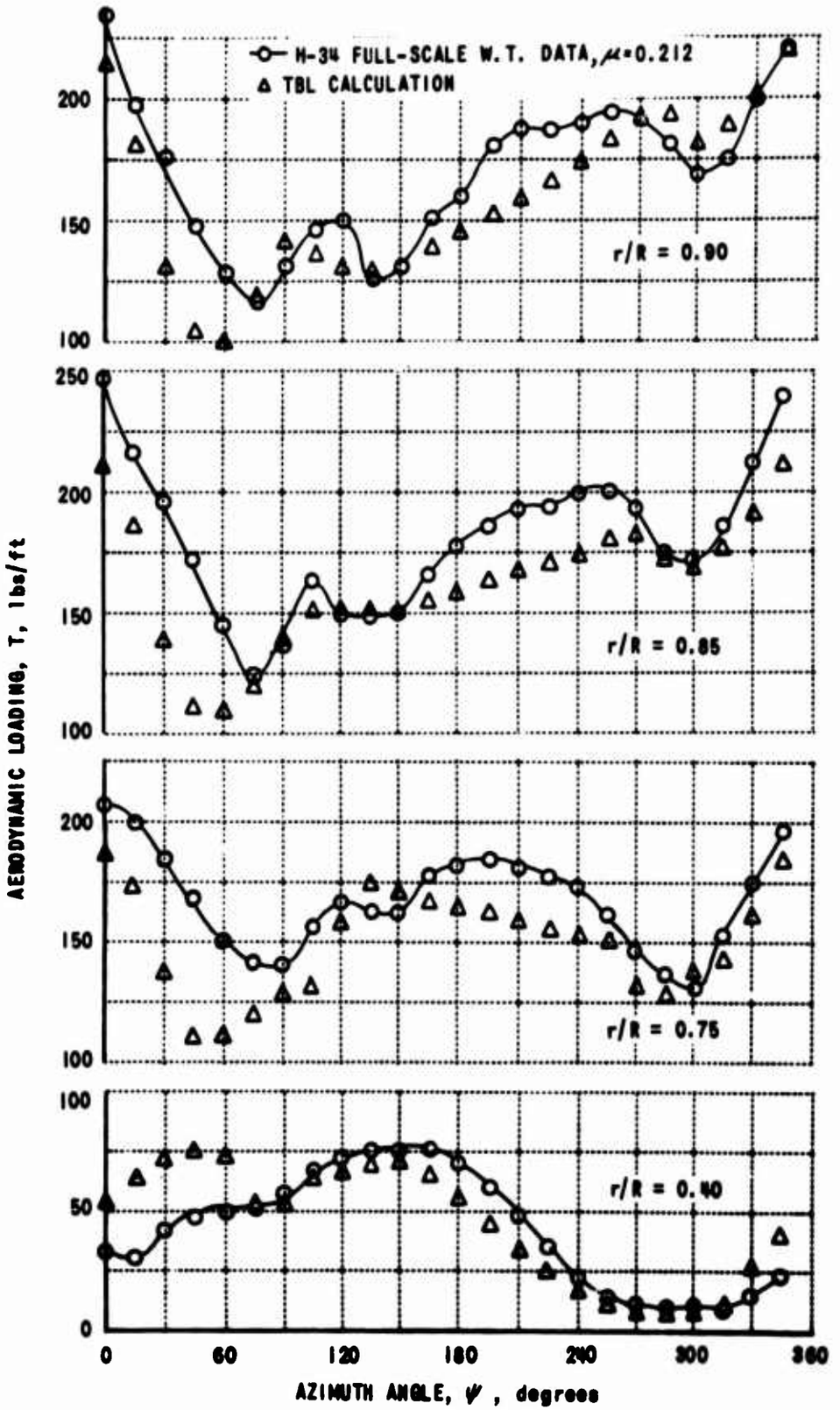

Figure 9. STEADY-STATE AERODYNAMIC LOADINGS vs. AZIMUTH ANGLE.

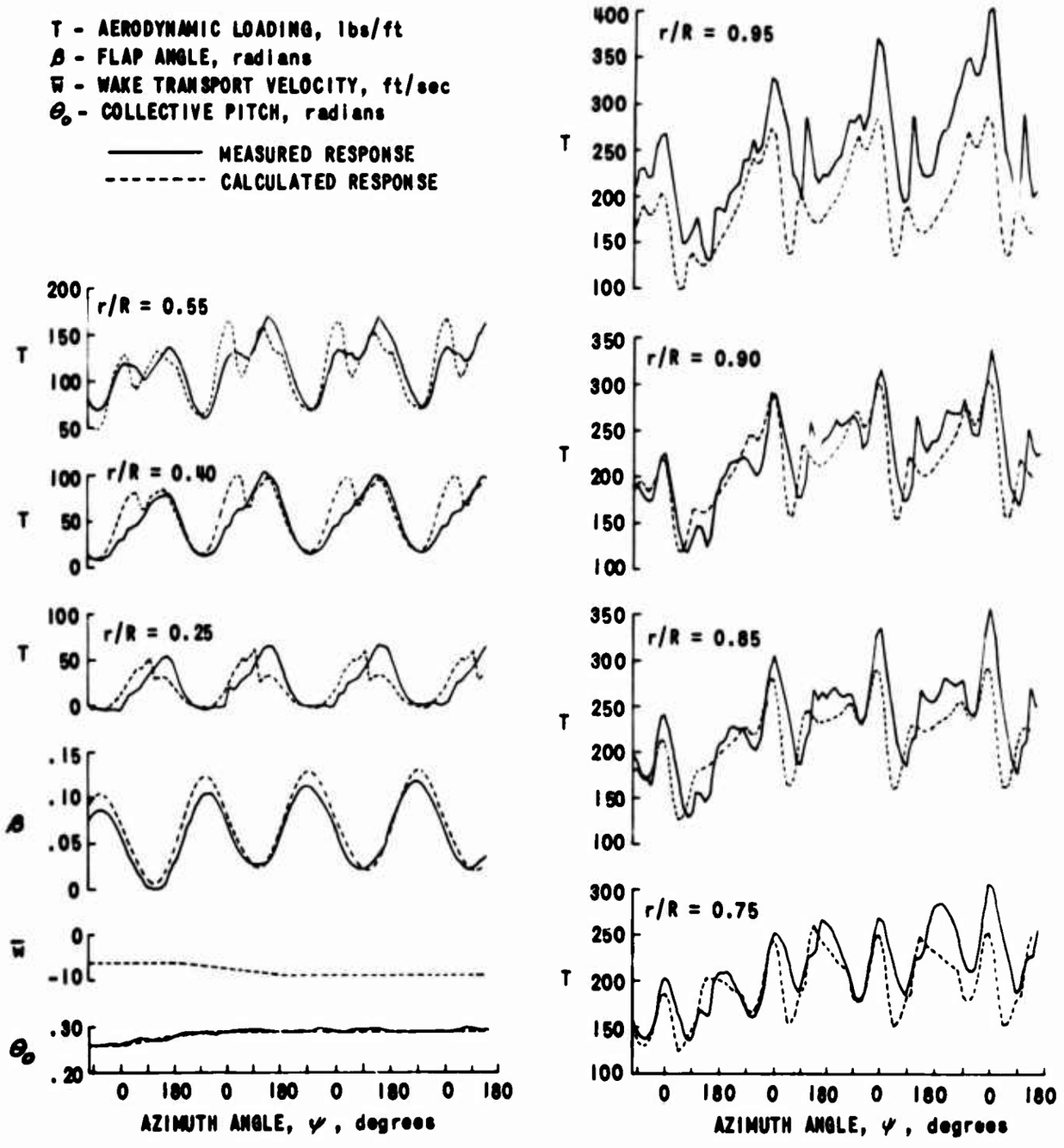

Figure 10. MEASURED AND CALCULATED TRANSIENT FLAPPING AND AIR LOAD RESPONSES; H-34 ROTOR, WIND-TUNNEL RUN 1, $\mu = 0.202$.

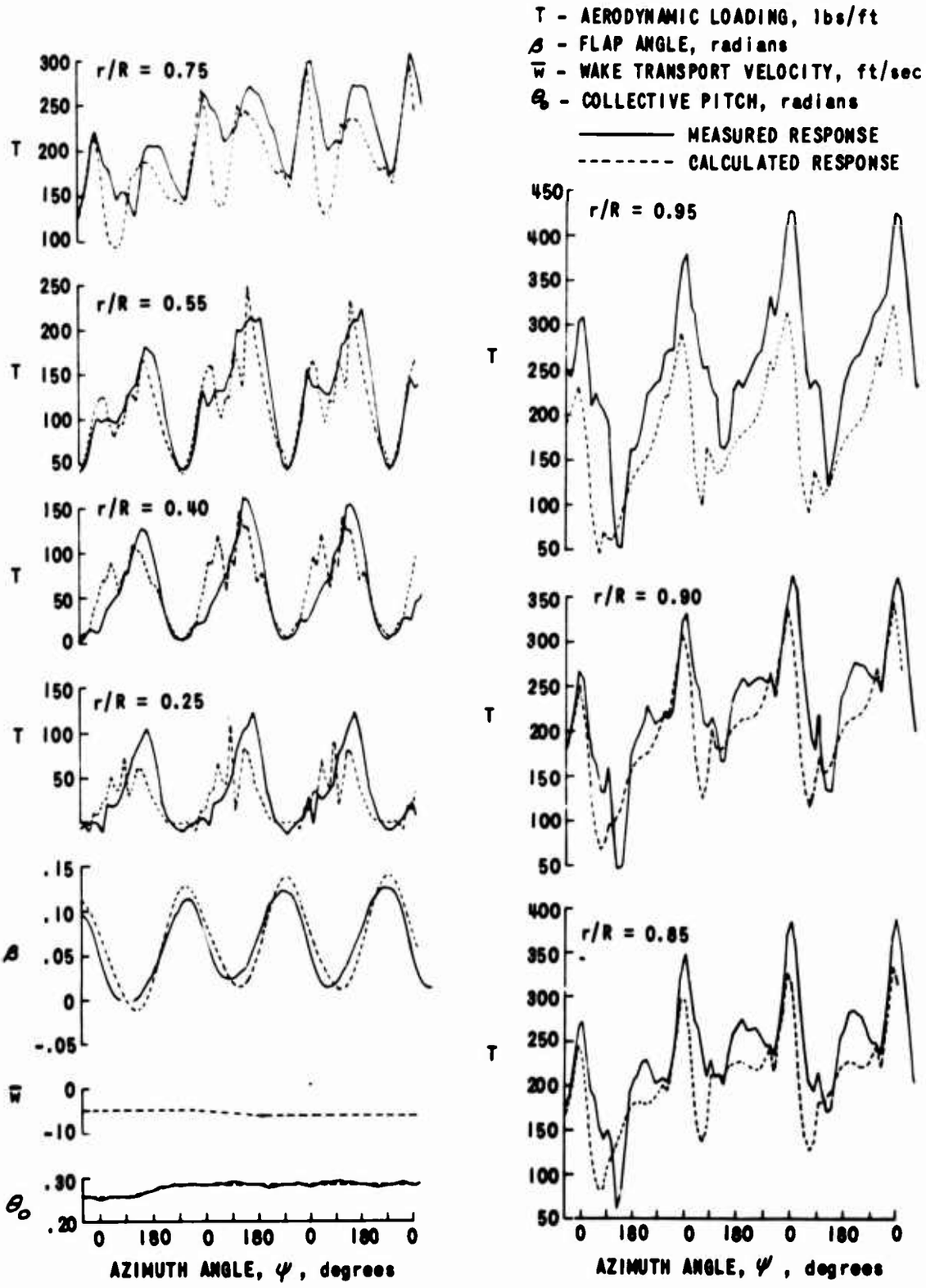

Figure 11. MEASURED AND CALCULATED TRANSIENT FLAPPING AND AIR LOAD RESPONSES; H-34 ROTOR, WIND-TUNNEL RUN 2, μ = 0.286.

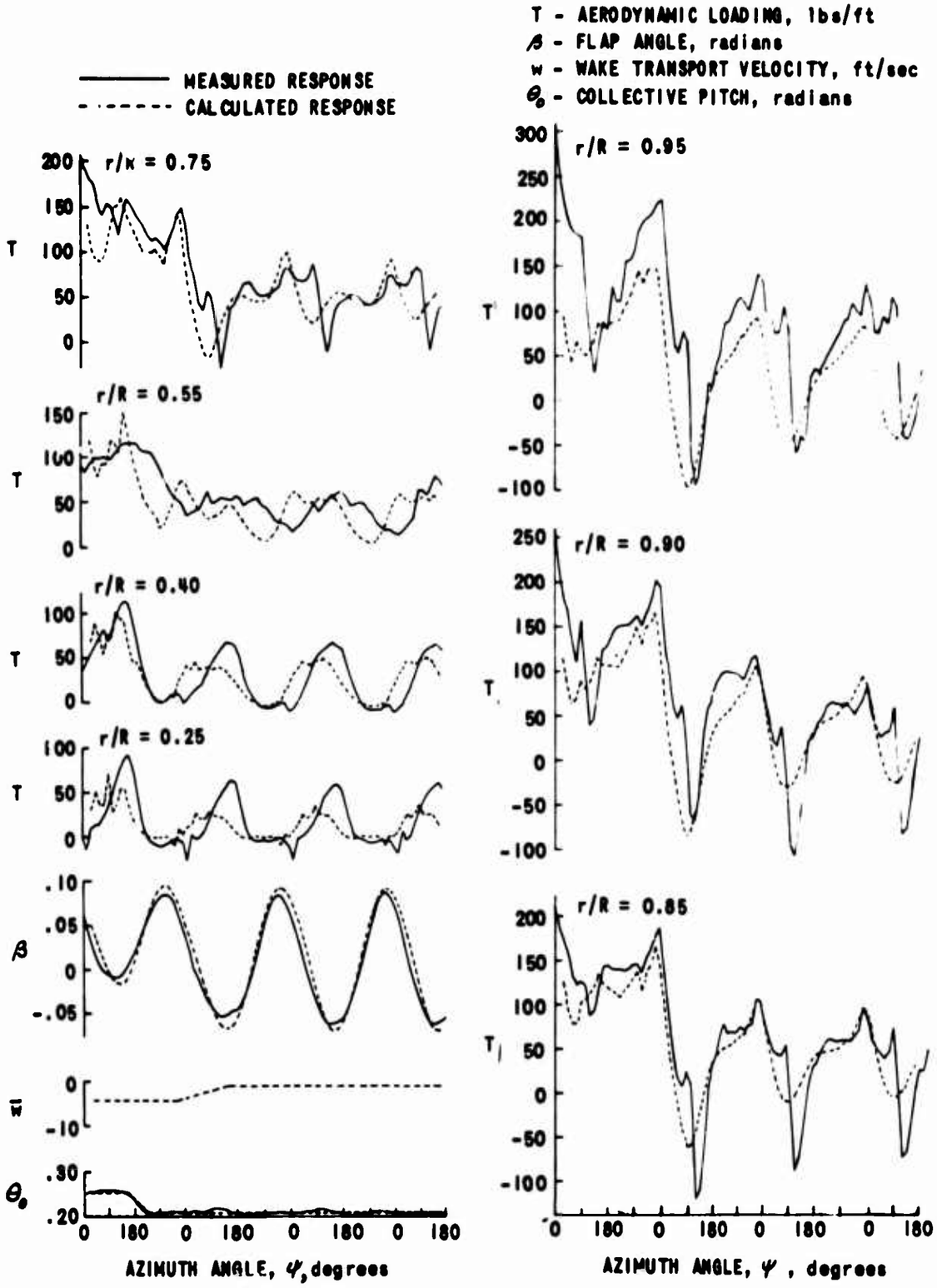

Figure 12. MEASURED AND CALCULATED TRANSIENT FLAPPING AND AIR LOAD RESPONSES; H-34 ROTOR, WIND-TUNNEL RUN 3, μ = 0.287.

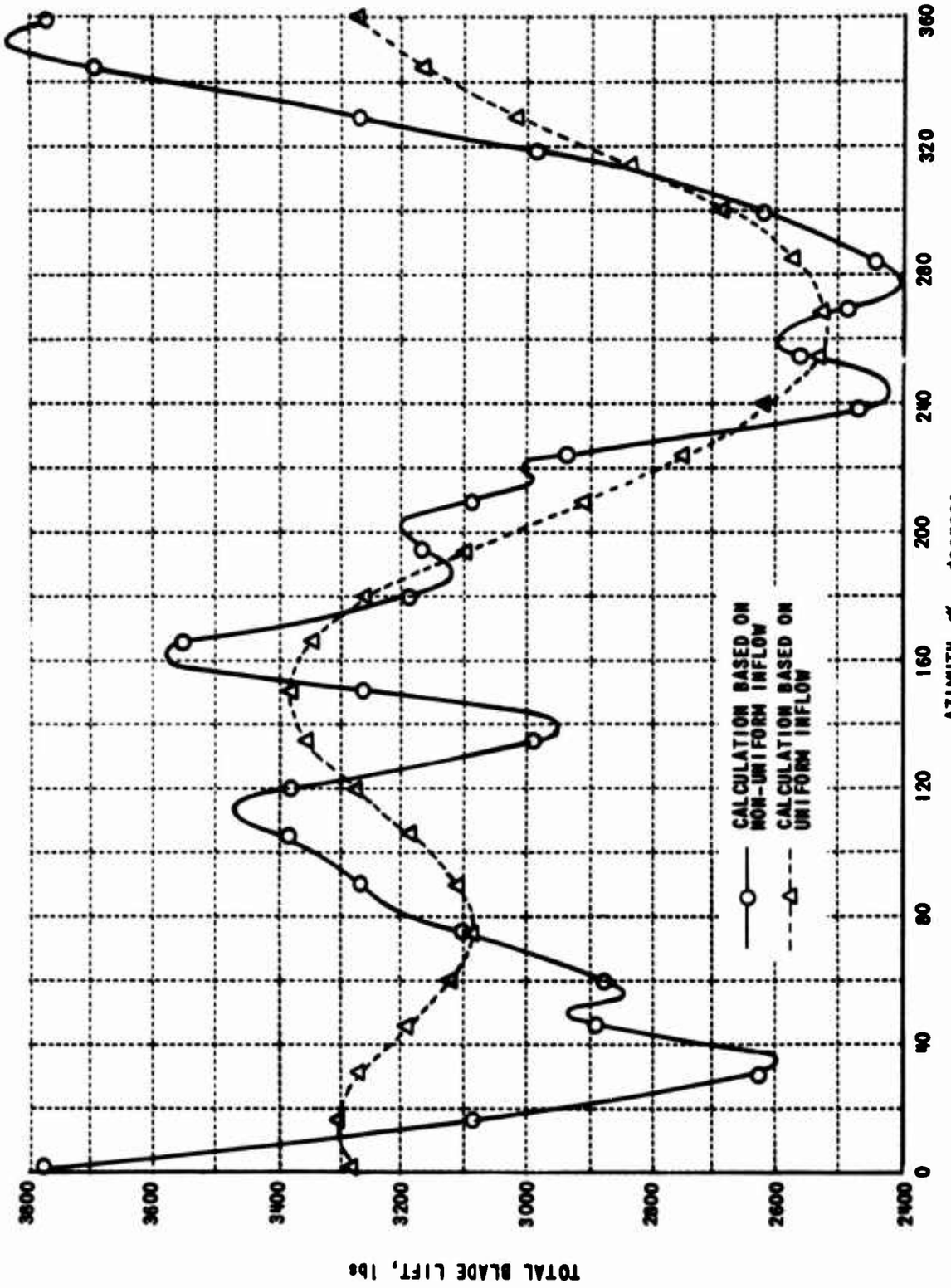

Figure 13. TOTAL LIFT ON BLADE vs. AZIMUTH; H-34 ROTOR, μ = 0.18.

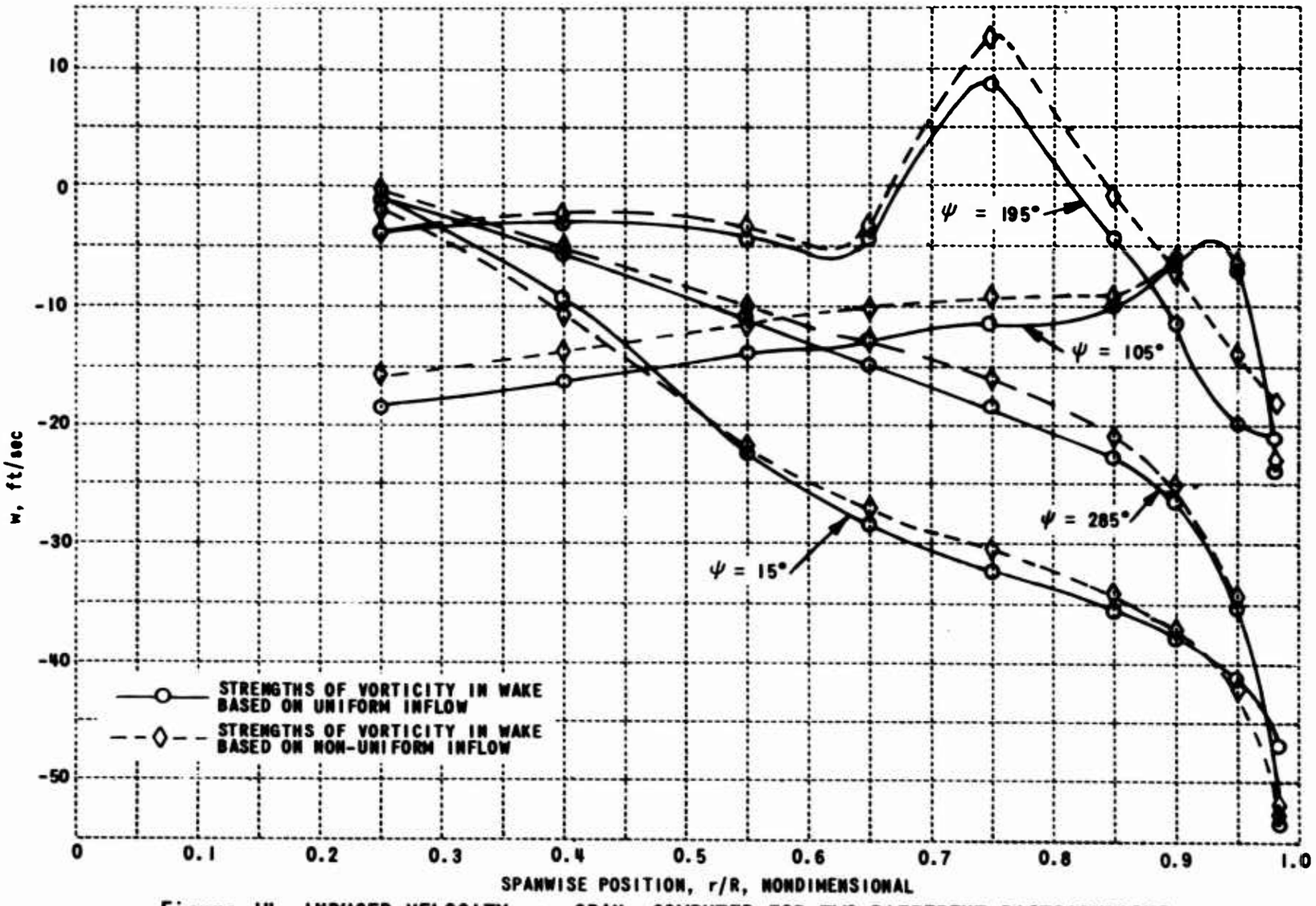

Figure 14. INDUCED VELOCITY vs. SPAN; COMPUTED FOR TWO DIFFERENT DISTRIBUTIONS OF VORTICITY IN THE WAKE; H-34 ROTOR, μ = 0.18.

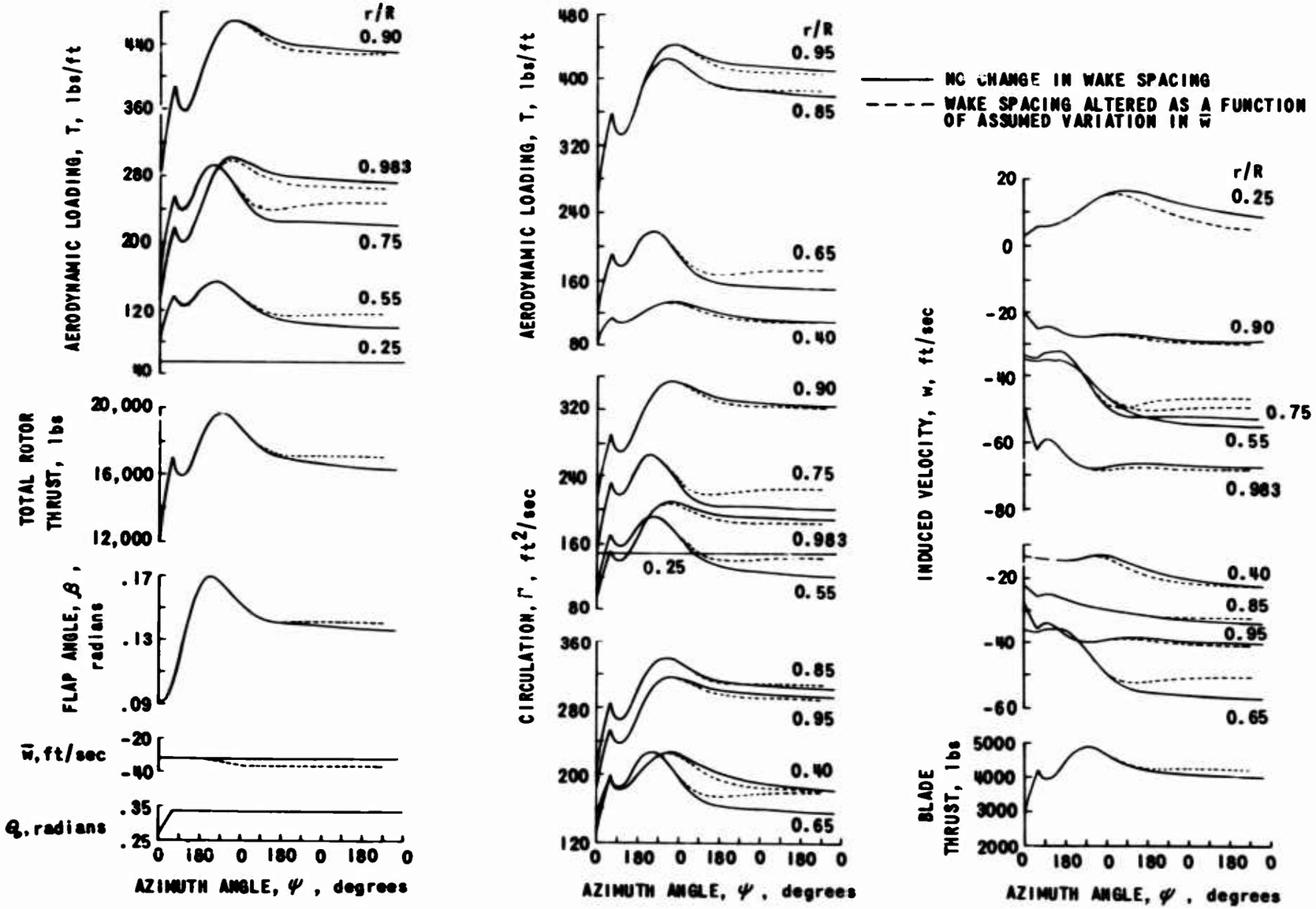

Figure 15. TRANSIENT RESPONSE TO A RAPID INCREASE IN COLLECTIVE PITCH; CALCULATED FOR THE H-34 ROTOR IN HOVERING FLIGHT.

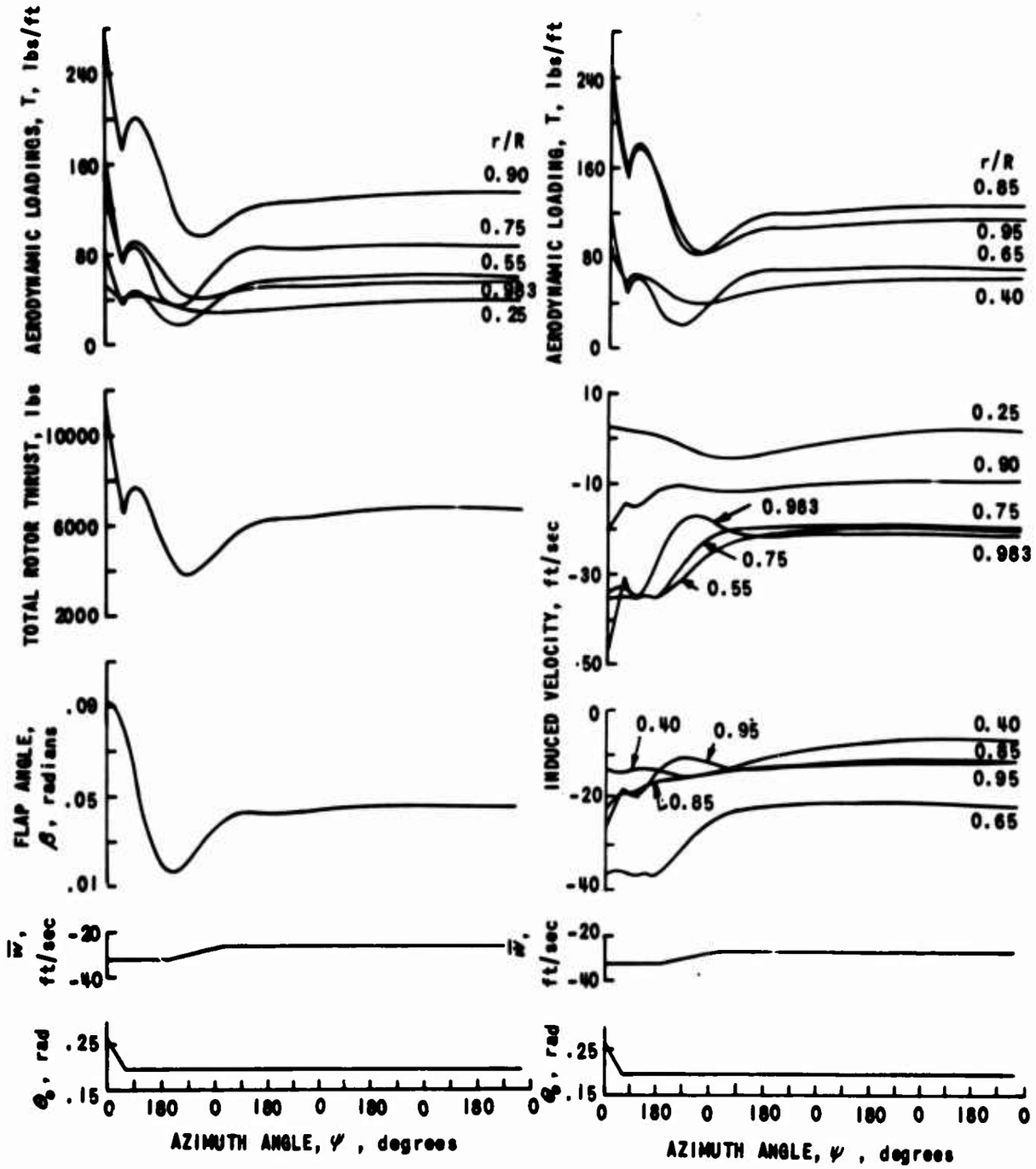

Figure 16. TRANSIENT RESPONSE TO A RAPID DECREASE IN COLLECTIVE PITCH; CALCULATED FOR THE H-34 ROTOR IN HOVERING FLIGHT.

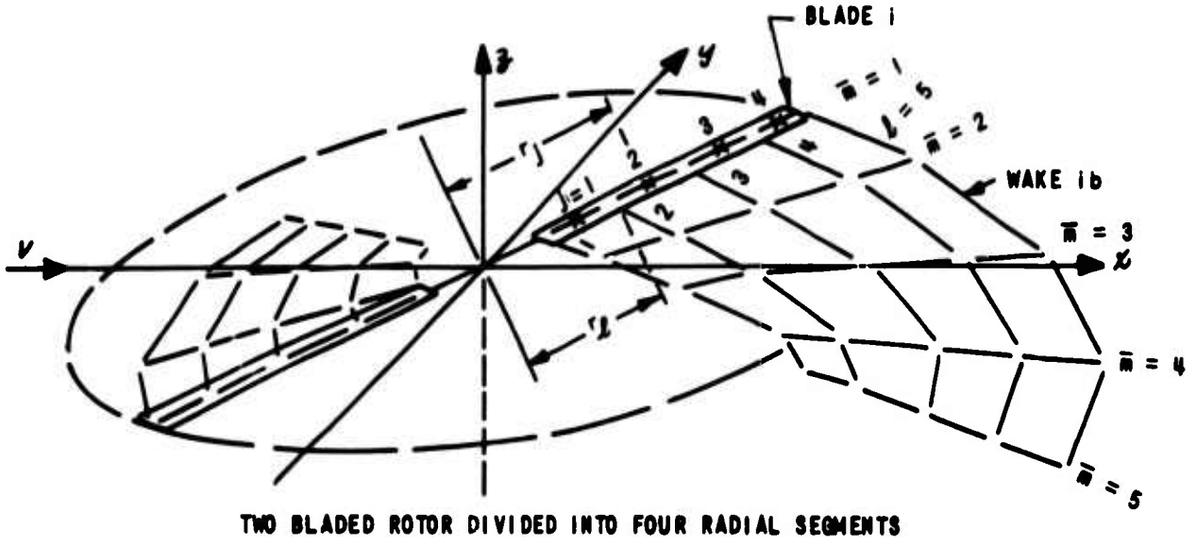

Figure 17. INDEXING PROCEDURE USED TO DESIGNATE BLADE AND WAKE GEOMETRY.

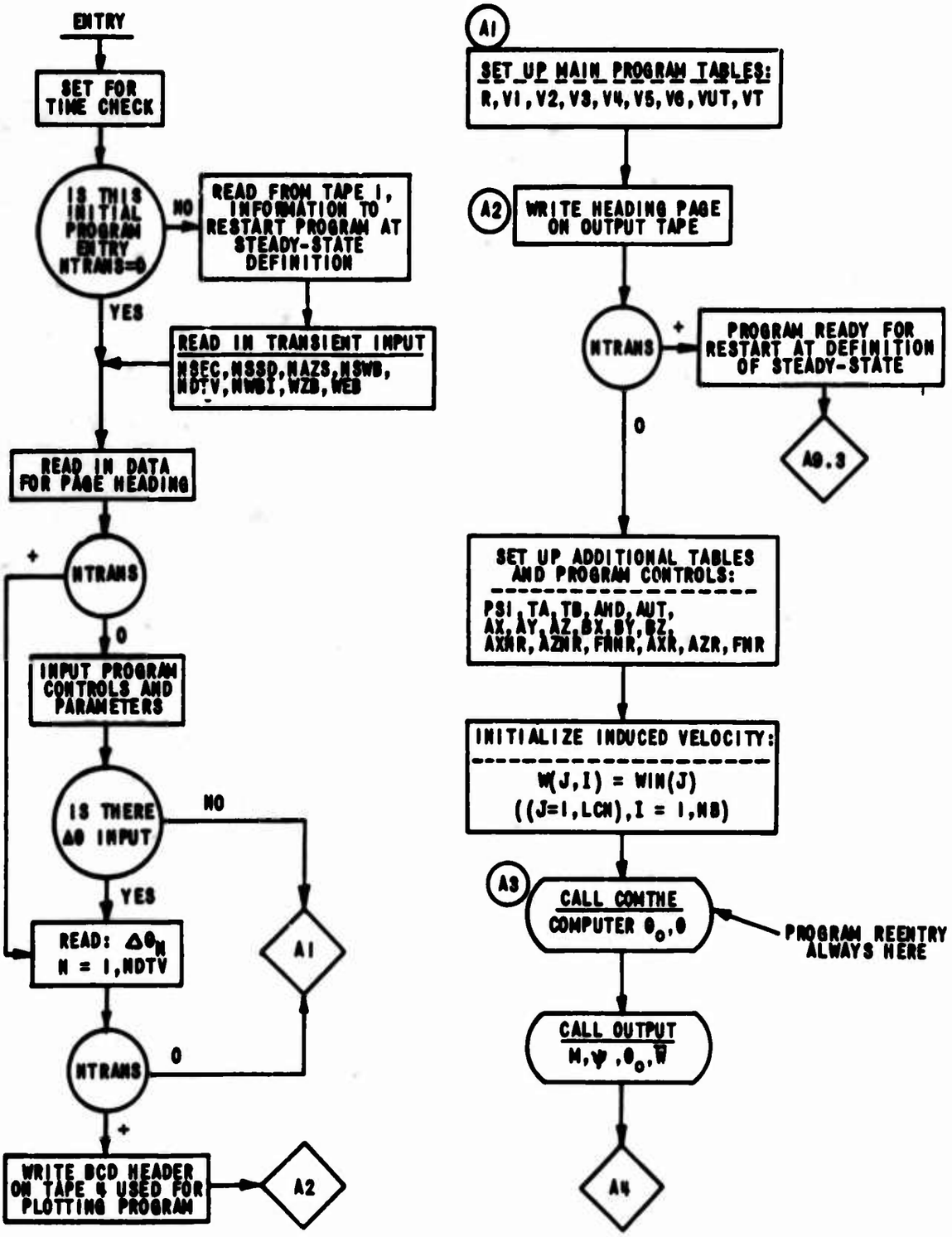

Figure 18(a). CONDENSED FLOW CHARTS: MAIN PROGRAM - "BLADES".

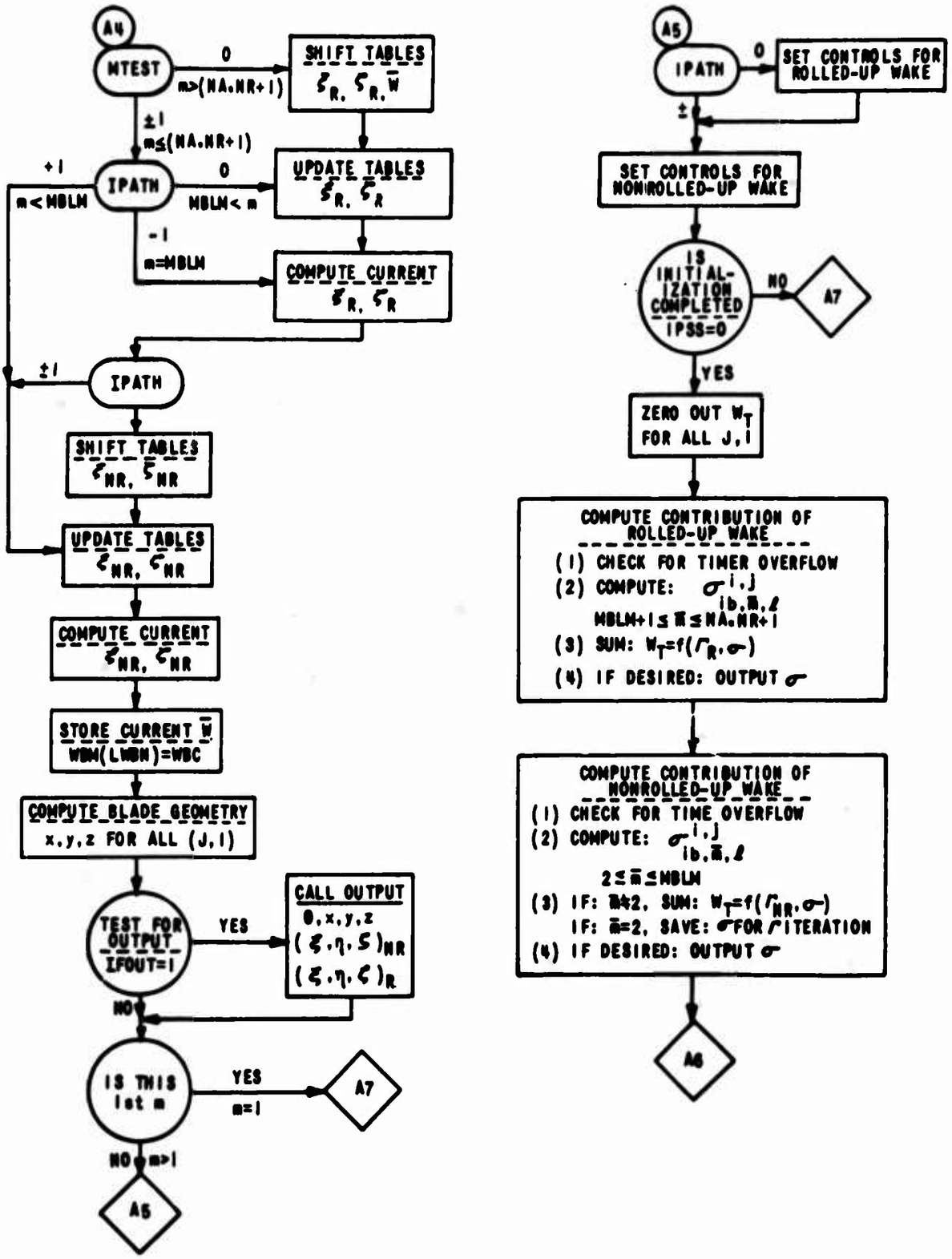

Figure 18(b). CONDENSED FLOW CHARTS: MAIN PROGRAM - "BLADES".

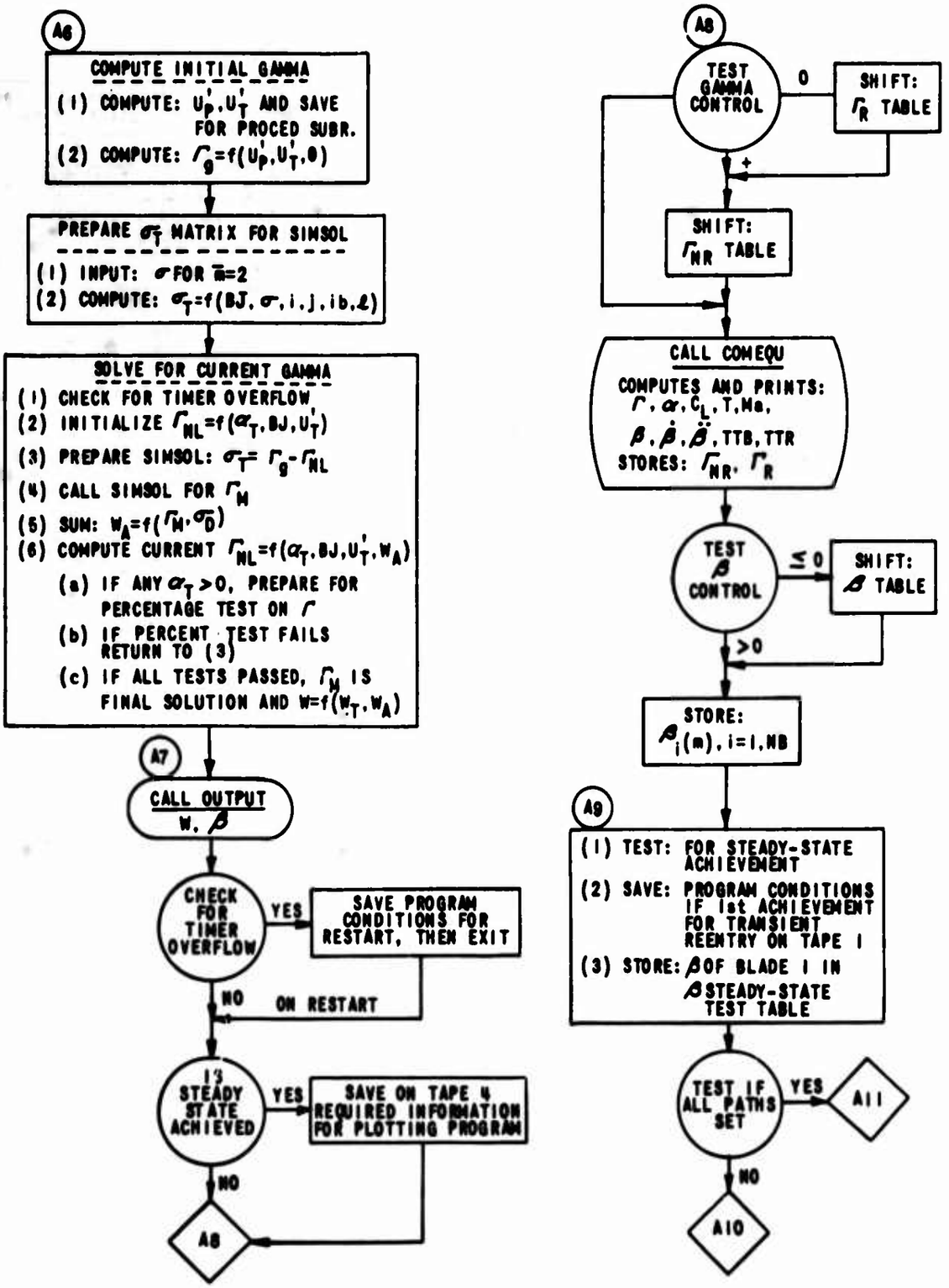

Figure 18(c). CONDENSED FLOW CHARTS: MAIN PROGRAM - "BLADES".

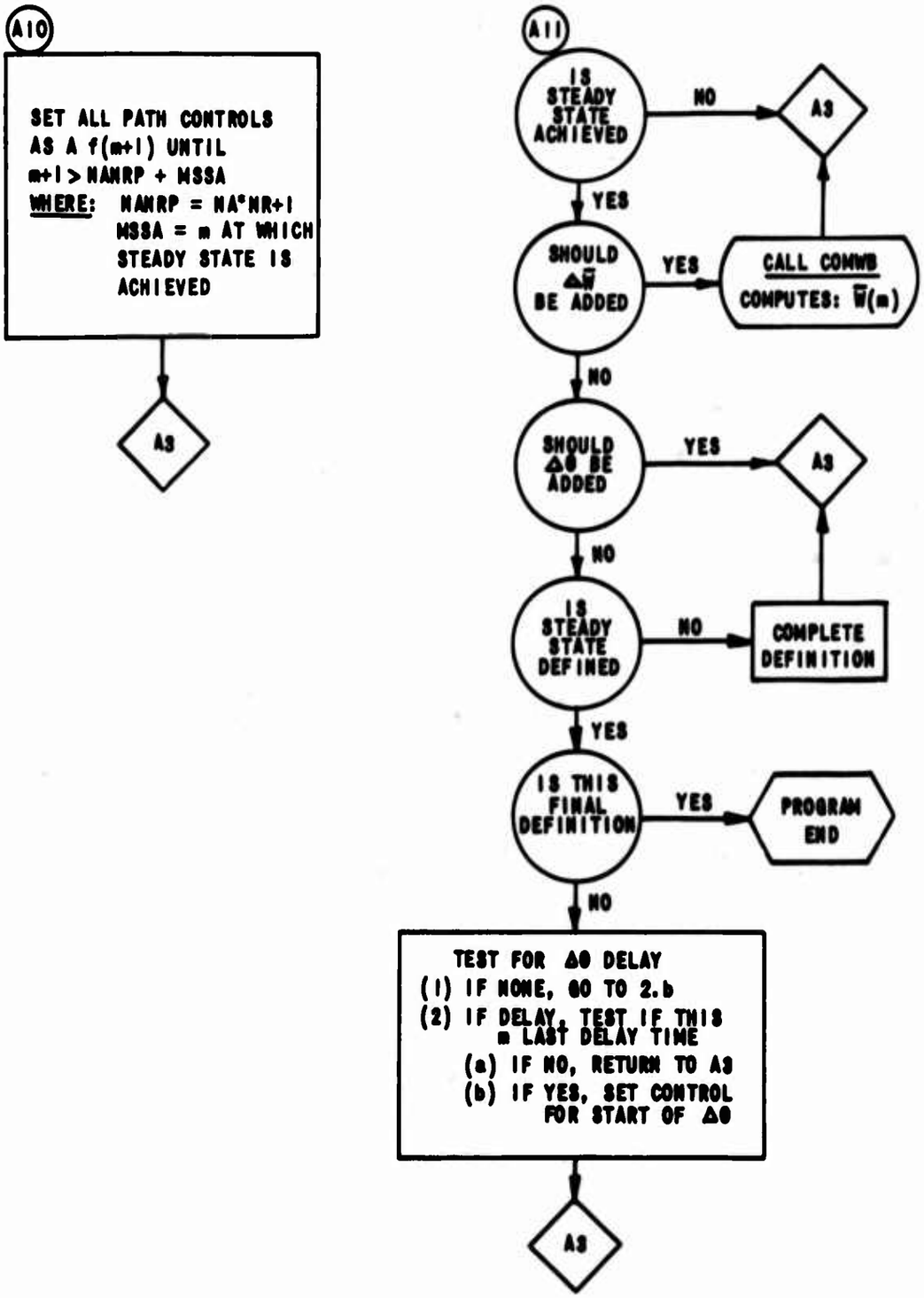

Figure 18(d). CONDENSED FLOW CHARTS: MAIN PROGRAM - "BLADES".

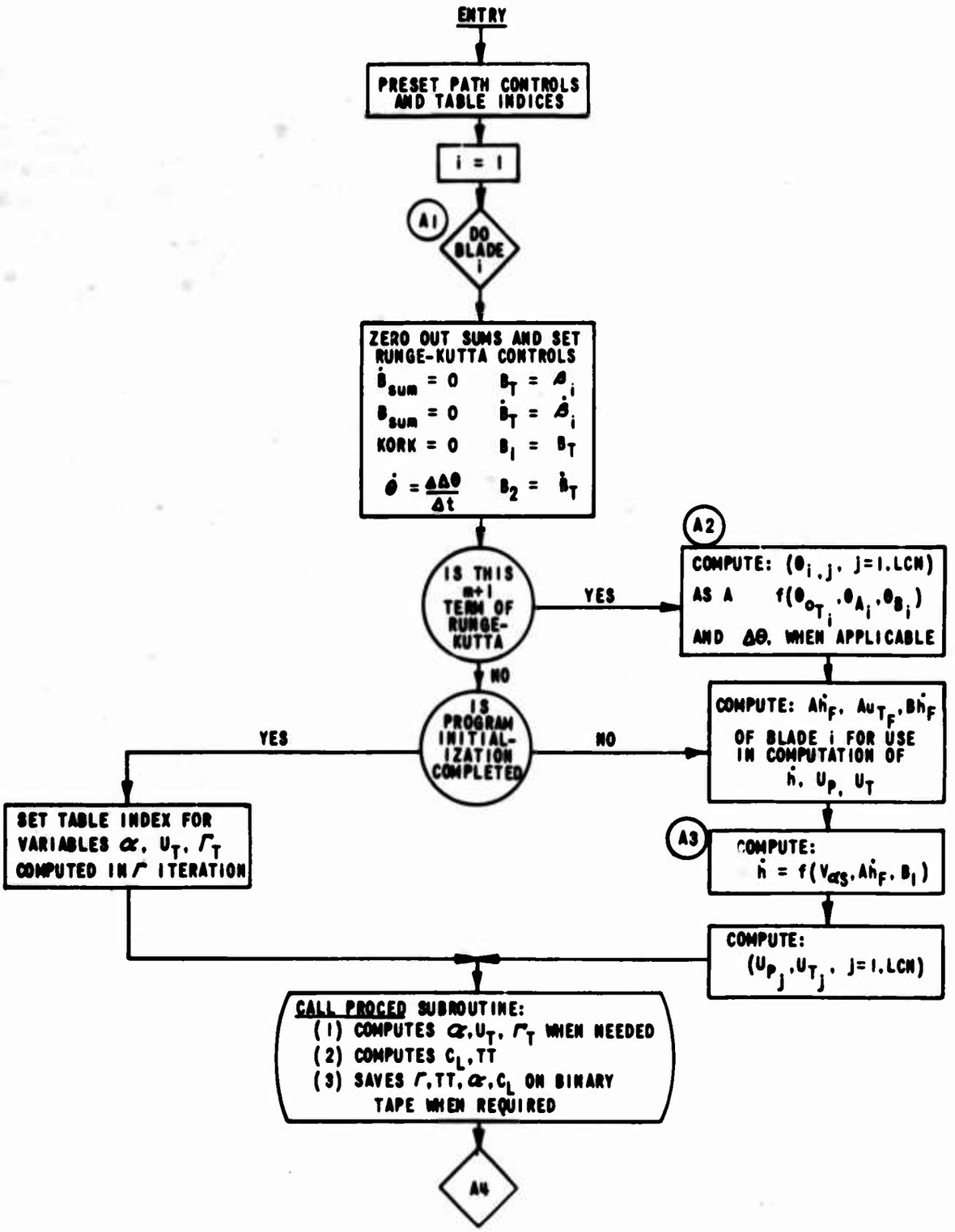

Figure 19(a). CONDENSED FLOW CHARTS: SUBROUTINE - "COMEQU".

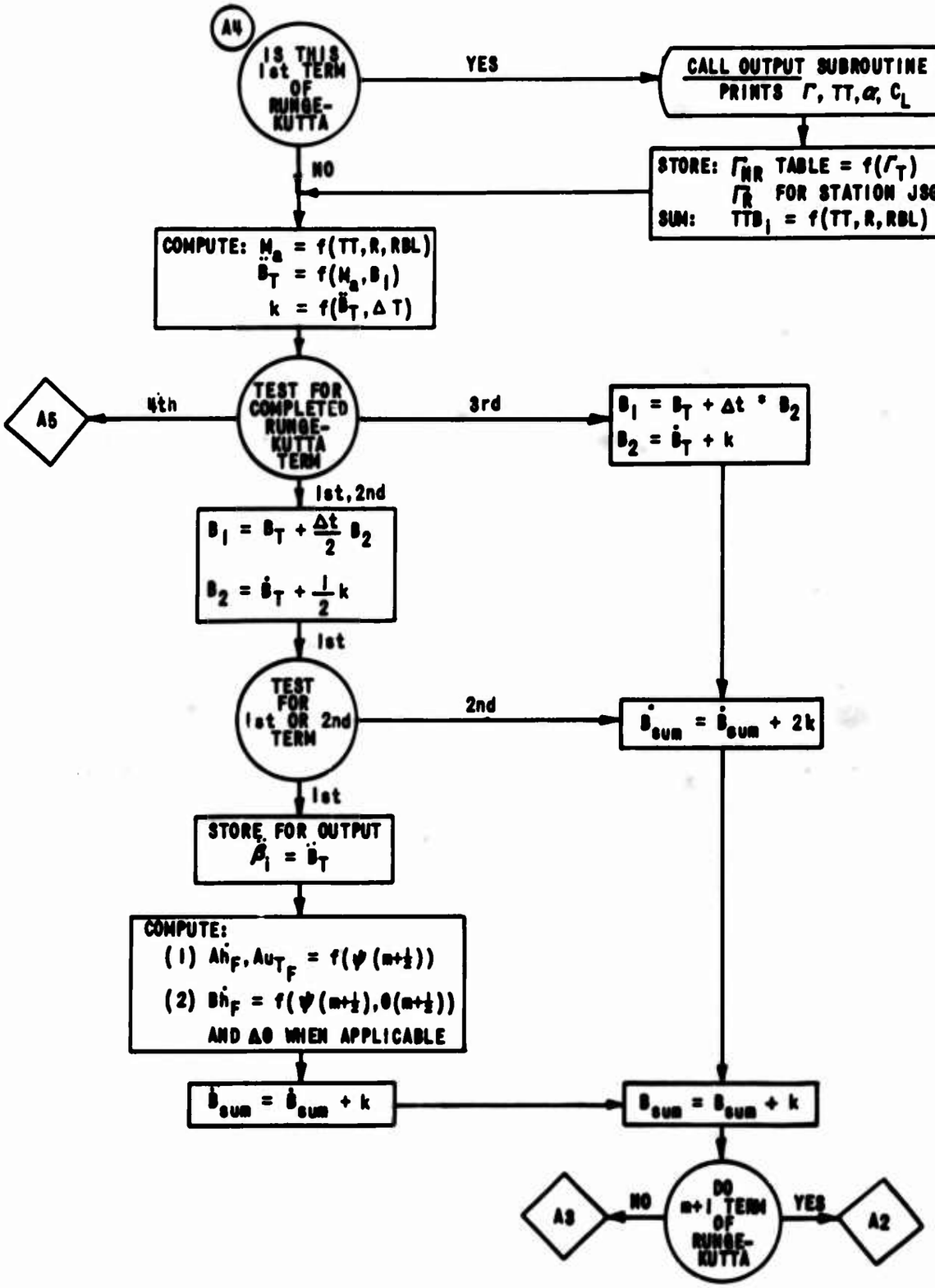

Figure 19(b). CONDENSED FLOW CHARTS: SUBROUTINE - "COMEQU".

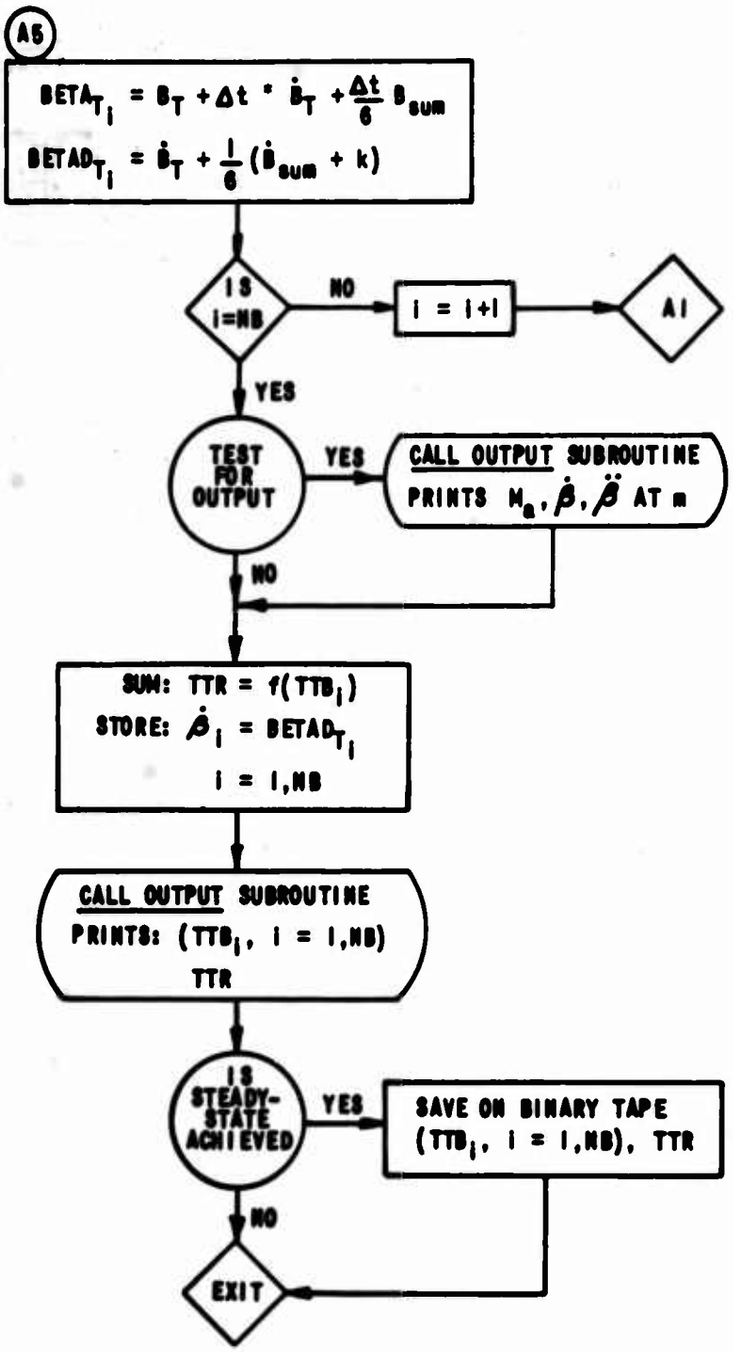

Figure 19(c). CONDENSED FLOW CHARTS: SUBROUTINE - "COMEQU".

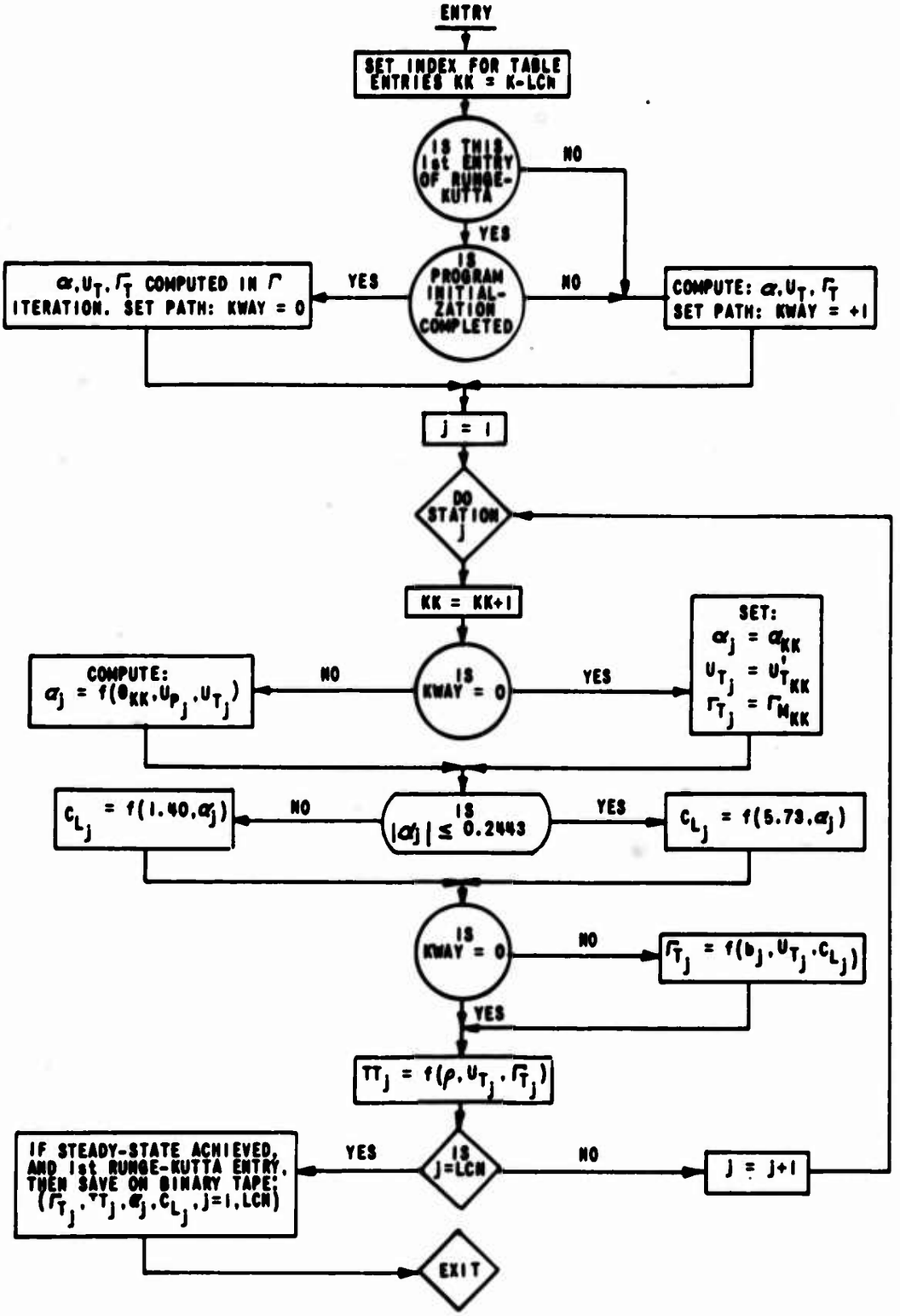

Figure 20. CONDENSED FLOW CHART: SUBROUTINE - "PROCED".

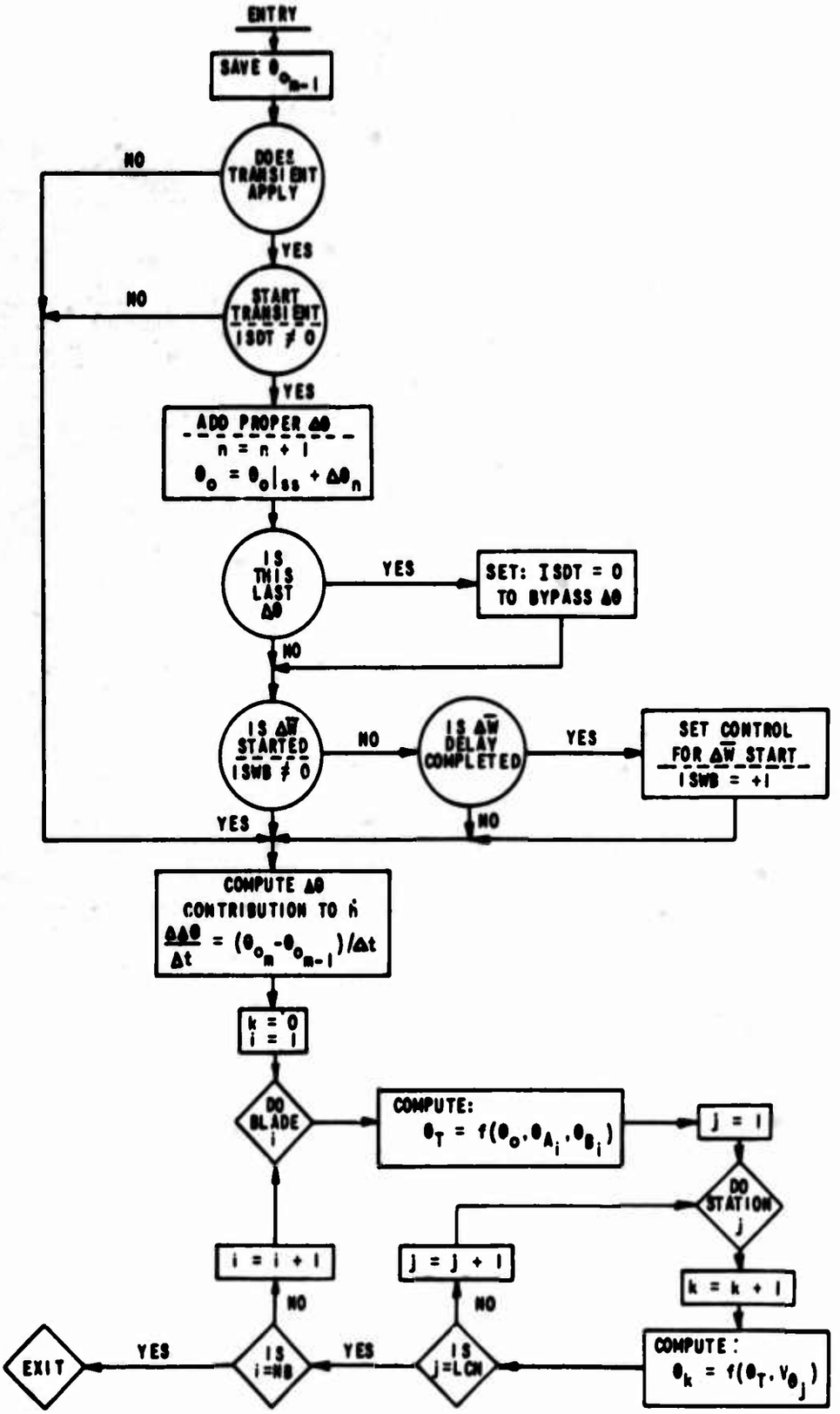

Figure 21. CONDENSED FLOW CHART: SUBROUTINE - "COMTHE".

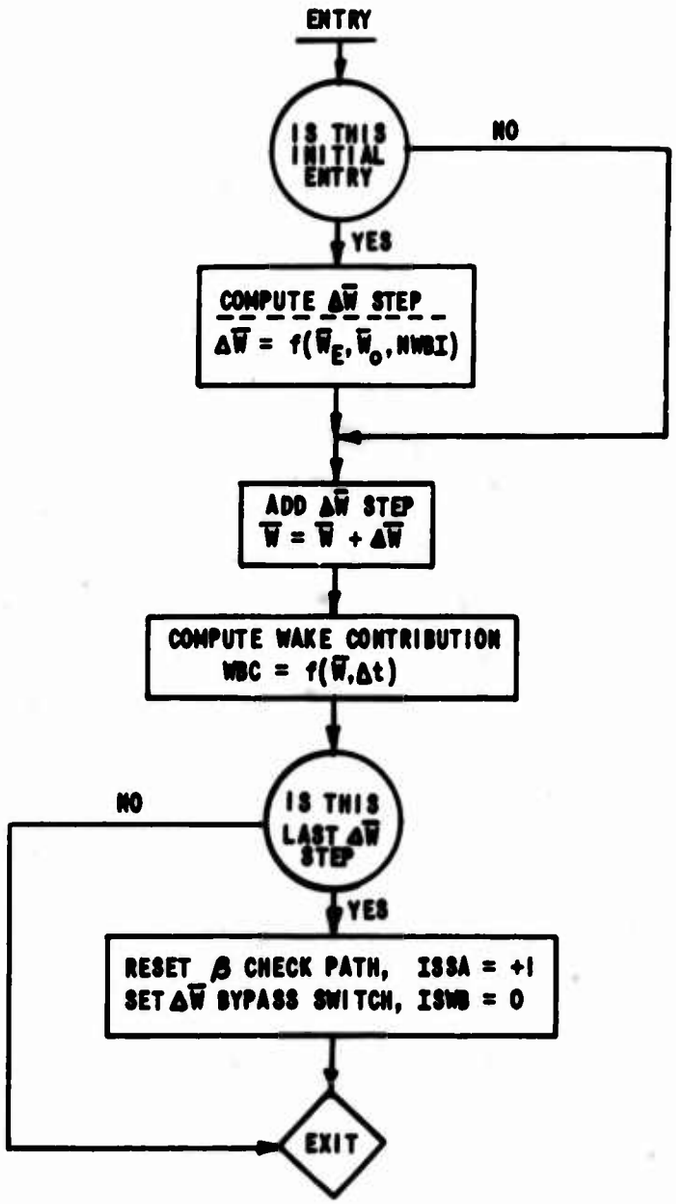

Figure 22. CONDENSED FLOW CHART: SUBROUTINE - "COMWB".

REFERENCES

1. Willmer, M. A. P., The Loading of Helicopter Blades in Forward Flight, ARC 21, 233, April 1959.

2. Molyneux, W. G., "An Approximate Theoretical Approach for the Determination of Oscillatory Aerodynamic Coefficients for a Helicopter Rotor in Forward Flight", The Aeronautical Quarterly, Volume XIII, Part 3, August 1962.

3. Miller, R. H., "On the Computation of Airloads Acting on Rotor Blades in Forward Flight", Journal of the American Helicopter Society, Volume 7, Number 2, 1962.

4. Miller, R. H., "Rotor Blade Harmonic Airloading", American Institute of Astronautics and Aeronautics Journal, Volume 2, Number 7, July 1964.

5. Miller, R. H., "Unsteady Airloads on Helicopter Rotor Blades", Journal of the Royal Aeronautical Society, Volume 68, Number 640, April 1964.

6. Tararine, S. and Delest, M., Experimental and Theoretical Study of Local Induced Velocity Over a Rotor Disc for Analytical Evaluation of the Primary Loads Acting on Helicopter Rotor Blades, Giravions Dorand Report Number DE 2012, 1960.

7. Shi-Tsun, Van, The Aerodynamic Characteristics of a Loaded Helicopter Rotor from a Three-Dimensional Vortex System, Aviotsionnaya Tekhnika, Number 1, 1961. (Translated by Willmer, M. A. P. and published as Library Translation Number 1013, Royal Aircraft Establishment.)

8. Shi-Tsun, Van, Generalized Vorticity Theory of Helicopter Lifting Rotors, United States Air Force, Foreign Technology Division, Technical Translation 62-185.

9. Davenport, F. J., "A Method for Computation of the Induced Velocity Field of a Rotor in Forward Flight, Suitable for Application to Tandem Rotor Configurations", Journal of the American Helicopter Society, Volume 9, Number 3, July 1964.

10. Piziali, R. A. and DuWaldt, F. A., Computation of Rotary Wing Harmonic Airloads and Comparison with Experimental Results, Proceedings of the American Helicopter Society Eighteenth Annual National Forum, 1962.

11. Piziali, R. A. and DuWaldt, F. A., Computed Induced Velocity Induced Drag, and Angle of Attack Distributions for a Two-Bladed Rotor, Proceedings of the American Helicopter Society Nineteenth Annual National Forum, 1963.

12. Piziali, R. A. and DuWaldt, F. A., A Method for Computing Rotary Wing Airload Distribution in Forward Flight, Report TCREC TR-62-44, U. S. Army Aviation Materiel Laboratories, Ft. Eustis; Virginia, * November 1962.

13. Carpenter, R. J. and Fridovich, B., Effect of a Rapid Blade-Pitch Increase on the Thrust and Induced-Velocity Response of a Full-Scale Helicopter Rotor, National Advisory Committee for Aeronautics TN 3044, November 1953.

14. Rebont, J., Valensi, J., and Soulez-Lariviere, J., Response of a Helicopter Rotor to an Increase in Collective Pitch for the Case of Vertical Flight, National Aeronautics and Space Administration Technical Translation F-55, January 1961.

15. Michel, D., Polleys, E., and Berman, A., Dynamic Response of a Helicopter to a Gust, Kaman Aircraft Corporation Report R-30, Part I, February 1957.

16. McCarty, J. L., Brooks, G. W., and Magliere, D. J., A Dynamic Model Investigation of the Effect of a Sharp-Edge Gust on Blade Periodic Flapping Angles and Bending Moments of a Two-Blade Rotor, National Aeronautics and Space Administration TN D-31, September 1959.

17. Gessow, A., and Crim, A. D., A Method for Studying the Transient Blade-Flapping Behavior of Lifting Rotors at Extreme Operating Conditions, National Advisory Committee for Aeronautics TN 3366, January 1955.

18. Burpo, F. B., and Lynn, R. R., Measurement of Dynamic Airloads on a Full-Scale Semi-Rigid Rotor, U. S. Army Aviation Materiel Laboratories, Ft. Eustis, Virginia, * December 1962.

19. Piziali, R. A., Prediction of Aerodynamic Loads and Motions of Rotor Blades, USAAVLABS Report, (to be published by U. S. Army Aviation Materiel Laboratories, Ft. Eustis, Virginia.)*

---

* Formerly, U. S. Army Transportation Research Command.

20. Scheiman, J., A Tabulation of Helicopter Rotor-Blade Differential Pressures, Stresses, and Motions as Measured in Flight, National Aeronautics and Space Administration TM X-952, March 1964.

21. Scheiman, J., and Ludi, L. H., Effect of Helicopter Rotor-Blade Tip Vortex on Blade Airloads, National Aeronautics and Space Administration TN D-1637, May 1963.

22. CH-34 Rotor Data obtained in NASA-Ames Wind Tunnel, 8 October 1964. (Tests performed by Sikorsky Aircraft Corporation under contract to USAAVLABS and provided to CAL by a personal communication from Sikorsky.)

23. Tanner, W. H., Charts for Estimating Rotary Wing Performance in Hover and at High Forward Speeds, National Aeronautics and Space Administration Contractor Report 114, November 1964.

24. Queijo, M. J., Theoretical Span Load Distributions and Rolling Moments for Sideslipping Wings of Arbitrary Plan Form in Incompressible Flow, National Advisory Committee for Aeronautics Technical Report 1269, 1956.

25. Weissinger, J., Der schiebende Tragflugel bei gesunder Stromung, Bericht S 2 der Lilienthal-Gesellschaft fur Luftfahrtforschung, 1938-1939.

APPENDIX

THE MATHEMATICAL MODEL AND COMPUTATIONAL PROCEDURE USED TO CALCULATE TRANSIENT BLADE LOADS

INDEXING NOMENCLATURE

A concise format for the equations forming the mathematical analog of a multibladed rotor generating a vortical wake requires the use of six indices. These indices are used both as subscripts and superscripts with the variables in the equations. Their purpose is to designate the time and spatial dependence of each variable under consideration.

The indices are m, i, j, ib, $\bar{m}$, and ℓ. They designate, respectively (1) an instant of time, (2) a blade of the rotor, (3) a spanwise location on a blade (corresponding to the midpoint of a designated segment), (4) the wake trailed by blade i, (5) an azimuthal position in the wake and (6) a spanwise position in the wake (corresponding to the endpoints of the segments into which the blades have been divided). Figure 17 pictures the manner in which these indices are used to designate blade and wake geometry, for example. Although the time index, m, does not appear on the Figure, it should be understood that a value of m is associated with the azimuthal position of a blade designated as the reference blade (usually blade $i = 1$) since time and azimuth are equivalent variables for a rotor rotating at a fixed r.p.m.

INPUT DATA

The input data required to compute transient air loadings fall into the following categories:

(1) Data specifying the geometry of the rotor and its wake, including the specification of the number of calculation points.

(2) Data specifying the equilibrium flight condition, including the trim values of collective and cyclic pitch.

(3) Data specifying the mass properties of the rotor.

(4) Starting values for flap angle, flapping angular velocity, and induced velocities.

(5) Data specifying the variation in collective pitch and in the mean, induced downwash with time.

(6) Data necessary to control the operational logic built into the digital-computing program.

WAKE-GEOMETRY COMPUTATIONS

The coordinates of the midpoints of the blade segments (at the three-quarter chord) in the adopted x-y-z axis system (Figure 6) are designated as $[x_{m,i,j} ; y_{m,i,j} ; z_{m,i,j}]$. Similarly, the coordinates of the endpoints of the elements of trailing vorticity, in this same axis system, are designated, as $[\xi_{m,ib,\bar{m},\ell} ; \eta_{m,ib,\bar{m},\ell} ; \zeta_{m,ib,\bar{m},\ell}]$. The azimuthal position in the wake at which the wake is assumed to roll up into two vortices (i.e., one at the blade tip and one at blade root) is designated as $\bar{m} = MBLM$. With this notation, it becomes convenient to write a separate set of equations defining the geometry of the nonrolled wake ($\bar{m} \leq MBLM$) and the rolled-up wake ($\bar{m} \geq MBLM$).

With the aid of the definitions of r_j and $\bar{r}_\ell$ (given in Figure 17) and of the nomenclature called out in Figure 6, and on further defining

$\bar{w}_m$ = mean induced downwash governing the vertical transport of the vorticity in the wake ($\bar{w}$ is a function of time)

$\bar{r}(\ell = 1, 2)$ = radial distance to spanwise location of rolled-up root and tip vortex,

we obtain the following set of equations for $[x, y, z]$ and $[\xi, \eta, \zeta]$:

[x, y, z] of Blade-Segment Midpoints (at 3/4 chord)

$$x_{m,i,j} = r_j \cos\psi_{m,i} + b_j \sin\psi_{m,i} - (r_j - \epsilon)\,\alpha_s\,\beta_{m,i}$$

$$y_{m,i,j} = r_j \sin\psi_{m,i} - b_j \cos\psi_{m,i}$$

$$z_{m,i,j} = (r_j - \epsilon)\beta_{m,i} - b_j\,\theta_{m,i,j} + r_j\,\alpha_s \cos\psi_{m,i} + b_j\,\alpha_s \sin\psi_{m,i}$$

[ξ, η, ζ] of Vortex-Segment Endpoints; Nonrolled Wake

$$\bar{m} \le MBLM\,; \quad \bar{m} \le m$$

$$\bar{m} = 1 : \quad \xi_{m,ib,\bar{m},l} = \bar{r}_l \cos\psi_{m,ib} - (\bar{r}_l - \epsilon)\,\alpha_s\,\beta_{m,ib}$$

$$\bar{m} > 1 : \quad \xi_{m,ib,\bar{m},l} = \xi_{m-1,ib,\bar{m}-1,l} + \frac{2\pi}{\Omega(NA)}\,V$$

$$\bar{m} \ge 1 : \quad \eta_{m,ib,\bar{m},l} = \bar{r}_l \sin\psi_{m-\bar{m}+1,ib}$$

$$\bar{m} = 1 : \quad \zeta_{m,ib,\bar{m},l} = (\bar{r}_l - \epsilon)\beta_{m,ib} + \bar{r}_l\,\alpha_s \cos\psi_{m,ib}$$

$$\bar{m} > 1 : \quad \zeta_{m,ib,\bar{m},l} = \zeta_{m-1,ib,\bar{m}-1,l} + \frac{2\pi}{\Omega(NA)}\,\bar{w}_{m-\bar{m}-1}$$

[ξ, η, ζ] of Vortex-Segment Endpoints; Rolled-Up Wake

$$MBLM \le \bar{m} \le NA(NR)+1 \; ; \; \bar{m} \le m$$

$$\bar{m} = MBLM: \; \xi_{m,ib,MBLM,\ell} = \bar{r}_\ell \cos\psi_{m-MBLM+1,ib} - (\bar{r}_\ell - \epsilon)\alpha_s \beta_{m-MBLM+1,ib} + (MBLM-1)\frac{2\pi}{\Omega(NA)} V$$

$$\bar{m} > MBLM: \; \xi_{m,ib,\bar{m},\ell} = \xi_{m-1,ib,\bar{m}-1,\ell} + \frac{2\pi}{\Omega(NA)} V$$

$$\bar{m} \ge MBLM: \; \eta_{m,ib,\bar{m},\ell} = \bar{r}_\ell \sin\psi_{m-\bar{m}+1,ib}$$

$$\bar{m} = MBLM: \; \zeta_{m,ib,MBLM,\ell} = (\bar{r}_\ell - \epsilon)\beta_{m-MBLM+1,ib} + \bar{r}_\ell \alpha_s \cos\psi_{m-MBLM+1,ib} + (MBLM-1)\frac{2\pi}{\Omega(NA)} \bar{w}_{m-MBLM+1}$$

$$\bar{m} > MBLM: \; \zeta_{m,ib,\bar{m},\ell} = \zeta_{m-1,ib,\bar{m}-1,\ell} + \frac{2\pi}{\Omega(NA)} \bar{w}_{m-\bar{m}+1}$$

where:

$$\psi_{m,ib} = \psi_{m,i} \; ; \; \beta_{m,ib} = \beta_{m,i}$$

$$\psi_{m-\bar{m}+1,ib} = \psi_{m-\bar{m}+1,i}$$

$$\psi_{m-MBLM+1,ib} = \psi_{m-MBLM+1,i}$$

$$\beta_{m-\bar{m}+1,ib} = \beta_{m-\bar{m}+1,i}$$

$$\beta_{m-MBLM+1,ib} = \beta_{m-MBLM+1,i}$$

COMPUTATION OF σ MATRIX

The Biot-Savart law yields the relationship

$$w = \sigma\gamma$$

for the velocity induced in the z direction by an arbitrarily oriented straight vortex filament of constant vortex strength, γ. The coefficient σ is a function only of the coordinates of the point where the velocity is being computed and the coordinates of the vortex filament endpoints, i. e.,

$$\sigma = f\left\{\left[x_{m,i,j} ; y_{m,i,j} ; z_{m,i,j}\right], \left[\xi_{m,ib,\bar{m},\ell} ; \eta_{m,ib,\bar{m},\ell} ; \zeta_{m,ib,\bar{m},\ell}\right]\right\}$$

A complete set of σ coefficients represents the influence of all of the elements of vorticity in the wake (of unit strength) at all of the load calculation points on each blade.

It is convenient to indicate the coefficient, σ, applicable to a specific element of trailing vorticity and to a specific segment calculation point as $\sigma^{m,i,j}_{ib,\bar{m},\ell}$. The superscripts, m, i, and j, indicate the specific location, as given by its $[x_{m,i,j} ; y_{m,i,j} ; z_{m,i,j}]$ coordinate, at which the induced velocity is being determined. The subscripts, ib, $\bar{m}$, and ℓ indicate the element of vorticity in the wake, as given by the $[\xi_{m,ib,\bar{m},\ell} ; \eta_{m,ib,\bar{m},\ell} ; \zeta_{m,ib,\bar{m},\ell}]$ coordinates at both the fore and aft ends of the element. The notation is such that the aft end of the vortex element is located at the azimuthal position, $\bar{m}$, with the forward end at the azimuthal position, $\bar{m} - 1$. Accordingly, no value can exist for $\sigma^{m,i,j}_{ib,\bar{m},\ell}$ when $\bar{m} = 1$.

For $m \geq 2$, application of the Biot-Savart law yield

$$\sigma^{m,i,j}_{ib,\bar{m},\ell} = \frac{(r_a + r_b)(l_a m_b - l_b m_a)}{4\pi r_a r_b (r_a r_b + l_a l_b + m_a m_b + n_a n_b)}$$

where

$$l_a = x_{m,i,j} - \xi_{m,ib,\bar{m},\ell}$$

$$m_a = y_{m,i,j} - \eta_{m,ib,\bar{m},\ell}$$

$$n_a = z_{m,i,j} - \zeta_{m,ib,\bar{m},\ell}$$

$$\ell_b = x_{m,i,j} - \xi_{m,ib,\bar{m}-1,\ell}$$

$$m_b = y_{m,i,j} - \eta_{m,ib,\bar{m}-1,\ell}$$

$$n_b = z_{m,i,j} - \zeta_{m,ib,\bar{m}-1,\ell}$$

$$r_a^2 = \ell_a^2 + m_a^2 + n_a^2$$

$$r_b^2 = \ell_b^2 + n_b^2 + n_b^2$$

The above formulation for σ is unnecessarily lengthly for vortex elements located at a large distance from a blade segment. Thus the above equation is used for $r_a^2 < r_{m_1}^2$, where r_{m_1} is an input quantity to the computer program. For

$$r_{m_1}^2 \le r_a^2 \le r_{m_2}^2 : \quad \sigma_{ib,\bar{m},\ell}^{m,i,j} = \frac{\ell_a m_b - \ell_b m_a}{4\pi r_a^3}$$

$$r_a^2 > r_{m_2}^2 : \quad \sigma_{ib,\bar{m},\ell}^{m,i,j} = 0$$

INDUCED-VELOCITY COMPUTATION

For purposes of implementing the TBL computation, the contributions of all vortex elements to the total velocity induced at a blade-segment location are summed over the entire wake with the exception of the elements located immediately adjacent to the blades. It should be noted that the vortex strengths of the latter elements are a function of the bound-vorticity distribution on the blade and, thus are unknown quantities prior to the determination of these bound vorticities.

Rather than require the program to search for the maximum value of circulation on the blade for eventual assignment of these strengths to the rolled-up root and tip vortices, we arbitrarily specify that the

circulations associated with a given spanwise segment be assigned to the rolled-up wake. Past experience is employed for guidance in selecting that spanwise segment which, on the average, sees the maximum circulation along the span. We designate the incomplete summation for the induced velocity as w_T and, in accordance with the above remarks, express w_T as:

$$w_{T_{m,i,j}} = \sum_{ib=1}^{NB} \left\{ \sum_{\bar{m}=3}^{MBLM} \sum_{\ell=1}^{LCN+1} \sigma_{ib,\bar{m},\ell}^{m,i,j} \left[\Gamma_{ib,m-\bar{m}+2,\ell} - \Gamma_{ib,m-\bar{m}+2,\ell-1} \right] + \sum_{\bar{m}=MBLM+1}^{NA(NR)+1} \Gamma_{ib,m-\bar{m}+2,JSG} \left[\sigma_{ib,\bar{m},1}^{m,i,j} - \sigma_{ib,\bar{m},2}^{m,i,j} \right] \right\}$$

where:

$$m \geq 2$$

and $\Gamma_{ib,m-\bar{m}+2,\ell} = \Gamma_{m',i,j}$ with $m' = m-\bar{m}+2,\ i = ib,\ i = \ell$

$\Gamma_{ib,m-\bar{m}+2,\ell-1} = \Gamma_{m',i,j}$ with $m' = m-\bar{m}+2,\ i = ib,\ j = \ell-1$

$\Gamma_{ib,m-\bar{m}+2,JSG} = \Gamma_{m',i,j}$ with $m' = m-\bar{m}+2,\ i = ib,\ j = JSG$

NB = number of blades

LCN = number of blade load points

NR = number of revolutions of wake

JSG = blade station associated with maximum circulation.

ROTOR KINEMATICS

For a given blade segment, j, located at a distance, r_j, from the center of rotation, the aerodynamic angle of attack, measured in a plane perpendicular to the blade span, can be expressed as

$$\alpha_{m,i,j} = \theta_{m,i,j} + \phi_{m,i,j}$$

where

$\theta_{m,i,j}$ is the geometric pitch angle of the blade section measured with respect to the shaft plane

and

$$\varphi_{m,i,j} = \tan^{-1} \frac{U_{P_{m,i,j}}}{U_{T_{m,i,j}}}$$

The "perpendicular" and "tangential" components of the airstream relative to the blade, at the three-quarter chord, are:

$$U_{P_{m,i,j}} = -V\alpha_s + w_{m,i,j} - u_{m,i,j}\alpha_s - \left[V + w_{m,i,j}\alpha_s + u_{m,i,j}\right]\beta_{m,i}\cos\psi_{m,i}$$

$$- v_{m,i,j}\beta_{m,i}\sin\psi_{m,i} - (r_j - e)\dot{\beta}_{m,i} + b_j\left\{\dot{\theta}_{0_m} - \Omega\left[\theta_{1c}\sin\psi_{m,i} - \theta_{1s}\cos\psi_{m,i}\right]\right\}$$

$$U_{T_{m,i,j}} = \left[V + w_{m,i,j}\alpha_s + u_{m,i,j}\right]\sin\psi_{m,i} - v_{m,i,j}\cos\psi_{m,i} + \Omega r_j$$

where

$u_{m,i,j}$; $v_{m,i,j}$; $w_{m,i,j}$ are the x, y, z components, respectively, of the velocity induced by the wake at time, m, at blade, i, and station, j.

$\dot{\theta}_{0_m}$ is the rate of change of collective pitch (a function of time)

θ_{1c} and θ_{1s} are the cosine and sine components of cyclic pitch, respectively,

and

α_s and β have been considered to be small angles.

It should be noted, that whereas some of the terms in the equation for U_P may be significant at very low advance ratios, at moderate flight speeds we have

$$u, v \ll V$$

$$w\alpha_s \ll V$$

$$u\beta, v\beta \ll V\alpha_s, w$$

The equations for U_P and U_T thus simplify to the following set:

$$U_{P_{m,i,j}} = -V\alpha_s + w_{m,i,j} - V\beta_{m,i}\cos\psi_{m,i} + (r_j - \epsilon)\dot{\beta}_{m,i} + b_j\left\{\dot{\theta}_{o_m} - \Omega\left[\theta_{1c}\sin\psi_{m,i} - \theta_{1s}\cos\psi_{m,i}\right]\right\}$$

$$U_{T_{m,i,j}} = V\sin\psi_{m,i} + \Omega r_j$$

As was done in Reference 12, the velocity component, U_P, is considered to consist of (1) the velocity induced by the wake, i.e., w, and (2) the velocity caused by the "effective plunging" velocity of the blade. Thus we have that

$$U_{P_{m,i,j}} = w_{m,i,j} - \dot{h}_{m,i,j}$$

where

$$\dot{h}_{m,i,j} = V\alpha_s + V\beta_{m,i}\cos\psi_{m,i} + (r_j - \epsilon)\dot{\beta}_{m,i} - b_j\left\{\dot{\theta}_{o_m} - \Omega\left[\theta_{1c}\sin\psi_{m,i} - \theta_{1s}\cos\psi_{m,i}\right]\right\}$$

Finally, we note that the geometric pitch angle, $\theta_{m,i,j}$, of a given blade segment is given by the following kinematic relationship:

$$\theta_{m,i,j} = \theta_{o_m} + \frac{\Delta\theta}{R} r_j + \theta_{1c}\cos\psi_{m,i} + \theta_{1s}\sin\psi_{m,i}$$

where

θ_{o_m} is the collective pitch setting at the blade root (or at any specified spanwise location) and

$\frac{\Delta\theta}{R}$ is the twist (assumed linear) of the blade (rad/ft)

SOLUTION PROCEDURE FOR UNKNOWN CIRCULATION STRENGTHS

As was discussed in the body of the report, the determination of the unknown bound vorticities, $\Gamma_{m,i,j}$, is facilitated by linearizing the rotor kinematics, namely by assuming that

$$\alpha_{m,i,j} = \tan^{-1}\frac{U_{P_{m,i,j}}}{U_{T_{m,i,j}}} = \frac{U_{P_{m,i,j}}}{U_{T_{m,i,j}}}$$

On so doing, we have that

$$\Gamma_{m,i,j} = b_j a \left[\left| U_{T_{m,i,j}} \right| \theta_{m,i,j} + U_{P_{m,i,j}} \frac{\left| U_{T_{m,i,j}} \right|}{U_{T_{m,i,j}}} \right]$$

where

$$a = \frac{dC_l}{d\alpha}$$ (considered as a constant with no m, i, or j dependency).

Since $U_{P_{m,i,j}}$ is a function of $W_{m,i,j}$ which, in turn, is a function of all the Γ_m (i.e., for all i and j), the above equation contains, in an implicit fashion, all of the unknown circulation strengths existing on the blades at time, m. A set of equations relating each $\Gamma_{m,i,j}$ to all of the $\Gamma_{m,i,j}$'s existing at time m, must thereby be solved simultaneously to determine the unknown circulation strengths.

In order to facilitate this simultaneous solution, we define several of the existing variables or quantities in terms of the accumulated contribution of the wake with the exception of the trailing elements adjacent to the blades. Thus, we employ the previously defined incomplete summation for the induced velocity to obtain the following expression for the bound circulations due to the following known quantities:

$$\Gamma_{g_{m,i,j}} = b_j a \left[\left| U_{T_{m,i,j}} \right| \theta_{T_{m,i,j}} + U'_{P_{m,i,j}} \frac{\left| U_{T_{m,i,j}} \right|}{U_{T_{m,i,j}}} \right]$$

where

$$U'_{P_{m,i,j}} = W_{T_{m,i,j}} - \dot{h}_{m,i,j} .$$

The equation for $\Gamma_{m,i,j}$ can now be written as

$$\Gamma_{m,i,j} = \Gamma_{g_{m,i,j}} + b_j a \sum_{ib=1}^{NB} \sum_{\ell=1}^{LCN} \Gamma_{m,ib,\ell} \left[\sigma_{ib,2,\ell}^{m,i,j} - \sigma_{ib,2,\ell+1}^{m,i,j} \right].$$

If we further define

$$\sigma_{ib,\ell}^{i,j} = -b_j a \left[\sigma_{ib,2,\ell}^{m,i,j} - \sigma_{ib,2,\ell+1}^{m,i,j} \right]$$

where

$$ib, \ell \neq i, j$$

and

$$\sigma_{i,j}^{i,j} = 1 - b_j a \left[\sigma_{ib=i,2,\ell=j}^{m,i,j} - \sigma_{ib=i,2,\ell+1=j+1}^{m,i,j} \right]$$

the $i \times j$ set of equations for $\Gamma_{m,i,j}$ can be written in matrix notation as

$$\left[\sigma_{ib,\ell}^{i,j} \right] \left\{ \Gamma_{m,i,j} \right\} = \left\{ \Gamma_{g_{m,i,j}} \right\}.$$

The desired solution can be expressed as

$$\left\{ \Gamma_{m,i,j} \right\} = \left[\sigma_{ib,\ell}^{i,j} \right]^{-1} \left\{ \Gamma_{g_{m,i,j}} \right\}.$$

This solution procedure (as outlined above) holds for a linear relationship between lift and angle of attack wherein no accounting is made for the influence or effects of aerodynamic stall. It is possible, however, to introduce the effect of stall in an approximate manner. In this study, it was assumed that $\alpha = 5.73$ and that the blade segments stall at fourteen degrees with the lift and circulation remaining equal to the value existing at $\alpha = 14$ degrees at any angle of attack in excess of fourteen degrees.

Bound circulations were limited to a maximum value by computing the angle of attack of each blade segment and introducing a limiting function on $\Gamma_{g_{m,i,j}}$. The blade segment angles of attack are:

$$\alpha_{m,i,j} = \theta_{m,i,j} + \frac{U_{P_{m,i,j}} + w_{A_{m,i,j}}}{U_{T_{m,i,j}}}$$

where the velocities induced by trailing elements adjacent to the blades are designated as $w_{A_{m,i,j}}$, and are given by

$$w_{A_{m,i,j}} = \sum_{ib=1}^{NB} \sum_{\ell=1}^{LCN} \Gamma_{m,ib,\ell} \left[\sigma_{ib,2,\ell}^{m,i,j} - \sigma_{ib,2,\ell+1}^{m,i,j} \right].$$

Note that $\Gamma_{m,ib,\ell}$ are unknown quantities until the equation set has been solved at least once. Accordingly, the $\alpha_{m,i,j}$ are first evaluated with $w_{A_{m,i,j}}$ assumed to be zero. If any of the initially determined $\alpha_{m,i,j}$ exceed the specified stall angle, we solve an equation set of the form

$$\left\{\Gamma_{m,i,j}\right\} = \left[\sigma^{i,j}_{ib,\ell}\right]^{-1}\left\{\Gamma_{g_{m,i,j}} - \Gamma_{NL_{m,i,j}}\right\}$$

where

$$\Gamma_{NL_{m,i,j}} = b_j \left|U_{T_{m,i,j}}\right| (\text{sign } \alpha_{m,i,j})\, a\left\{\left|\alpha_{m,i,j}\right| - \alpha_{stall}\right\}$$

subject to the requirement that

$$\left\{\left|\alpha_{m,i,j}\right| - \alpha_{stall}\right\} \geq 0$$

Only one solution of the simultaneous equation set is required if all the $\Gamma_{NL_{m,i,j}}$ are equal to zero. If this quantity exists, the equation set is solved and the $\Gamma_{NL_{m,i,j}}$ are redetermined. The solution procedure is repeated until the changes computed for $\Gamma_{m,i,j}$ are less than a specified percentage.

BLADE-FLAPPING DYNAMICS

The aerodynamic loading is designated as $T_{m,i,j}$ and under the assumptions made in the study can be expressed as

$$T_{m,i,j} = \rho U_{T_{m,i,j}} \Gamma_{m,i,j}$$

The moment about the flapping hinge caused by the aerodynamic loading, when expressed as a continuous function, is

$$M_{A_{m,i}} = \int_e^R (r-e)\, T(r)\, dr$$

and for the purposes of this study was numerically evaluated by means of a trapezoidal integration procedure. The resulting aerodynamic moments are used in the blade-flapping equation:

$$\ddot{\beta}_{m,i} = \frac{M_{Am,i}}{I_b} - \frac{M_w}{I_b} - \Omega^2 \left(1 + \frac{e}{g} \frac{M_w}{I_b}\right) \beta_{m,i}$$

to obtain the angular-flapping accelerations at each instant of time.

It should be noted that the Runge-Kutta integration procedure, used to integrate $\ddot{\beta}_{m,i}$ to yield $\dot{\beta}_{m+1,i}$ and $\beta_{m+1,i}$, utilized predictions over the half and full interval with $w_{T\,m,i,j}$ assumed to be constant over the time (azimuth) interval. No attempt was made to include the wake-geometry and induced-velocity computations into the Runge-Kutta integration since this procedure would have been prohibitive in terms of computing time and cost. Since the coupling between w_T and blade flapping during a single time interval is very small, the errors introduced by removing the w_T calculation from the Runge-Kutta procedure are believed to be negligible.

DIGITAL-COMPUTER PROGRAM

The above outlined mathematical model was programmed by means of the IBM FORTRAN IV language for the 7044 computer. The limited storage capacity of the 7044 required that a small portion of the coefficients be computed and then used immediately to compute their contribution to w_T. Since the σ coefficients for the elements adjacent to the blades must be saved for use in the simultaneous solution procedure, lack of sufficient storage capacity required that these coefficients be read out on tape. Although this requirement has been a significant factor in determining the computing time per azimuth interval, the major time-consuming portion of the program is the wake geometry and σ-calculation phase. For the case of a four-bladed rotor with three revolutions of wake, the program in its present form, requires approximately 0.64 minutes-per-azimuth interval when no iterations are required. Since 100 time intervals is a typical example of the number of intervals required to compute either a steady-state or transient response, a typical computation requires

approximately one hour.

Condensed flow charts for the main program and the subroutines are presented in Figures 18 through 22. These flow charts can be compared with Figure 5 to show the manner in which the developed mathematical analog was augmented with additional logic to facilitate numerical computations.

Unclassified

Security Classification

DOCUMENT CONTROL DATA - R&D

(Security classification of title, body of abstract and indexing annotation must be entered when the overall report is classified)

1. ORIGINATING ACTIVITY (Corporate author)

Cornell Aeronautical Laboratory, Inc.
Buffalo, New York 14221

2a. REPORT SECURITY CLASSIFICATION

Unclassified

2b. GROUP

3. REPORT TITLE

Air Loadings on a Rotary Wing as Caused by Transient Inputs of Collective Pitch

4. DESCRIPTIVE NOTES (Type of report and inclusive dates)

Final Report September 1963 through May 1965

5. AUTHOR(S) (Last name, first name, initial)

Segel, Leonard

6. REPORT DATE	7a. TOTAL NO. OF PAGES	7b. NO. OF REFS
October 1965	73	25

8a. CONTRACT OR GRANT NO.	9a. ORIGINATOR'S REPORT NUMBER(S)
DA 44-177-AMC-77(T)	USAAVLABS Technical Report No. 65-65
b. PROJECT NO. 1P125901A142	
c.	9b. OTHER REPORT NO(S) (Any other numbers that may be assigned this report) CAL Report No. BB-1840-S-1
d.	

10. AVAILABILITY/LIMITATION NOTICES

Qualified requesters may obtain copies of this report from DDC.
This report has been furnished to the Department of Commerce for sale to the public.

11. SUPPLEMENTARY NOTES	12. SPONSORING MILITARY ACTIVITY
	U. S. Army Aviation Materiel Laboratories Fort Eustis, Virginia 23604

13. ABSTRACT

A method and a computer program are developed for predicting the non-periodic air loads caused by control inputs applied to a rotary wing in forward flight. Use is made of a numerical description of the geometry and circulation strength of the vorticity in the wake to compute the time-varying, nonuniform-inflow field in the plane of the rotor disc. The method of approach is similar to that developed previously for the steady-state flight condition, the major difference being that the solution procedure lends itself to the treatment of transient phenomena, such as the non-periodic loadings caused by time-varying collective pitch.

Computed flapping and air load distributions are compared with transient data obtained in wind-tunnel tests on a full-scale H-34 rotor. In general, very encouraging agreement is found leading to the conclusion that calculation and prediction of nonperiodic loadings on rotary wings is a feasible task.

DD FORM 1 JAN 64 1473

Unclassified

Security Classification

14. KEY WORDS	LINK A		LINK B		LINK C	
	ROLE	WT	ROLE	WT	ROLE	WT
Helicopter VTOL Aerodynamics Fluid dynamics Rotor Blades Rotary wing Transient loads Pitch change Cyclic pitch Digital program						

INSTRUCTIONS

1. **ORIGINATING ACTIVITY:** Enter the name and address of the contractor, subcontractor, grantee, Department of Defense activity or other organization *(corporate author)* issuing the report.

2a. **REPORT SECURITY CLASSIFICATION:** Enter the overall security classification of the report. Indicate whether "Restricted Data" is included. Marking is to be in accordance with appropriate security regulations.

2b. **GROUP:** Automatic downgrading is specified in DoD Directive 5200.10 and Armed Forces Industrial Manual. Enter the group number. Also, when applicable, show that optional markings have been used for Group 3 and Group 4 as authorized.

3. **REPORT TITLE:** Enter the complete report title in all capital letters. Titles in all cases should be unclassified. If a meaningful title cannot be selected without classification, show title classification in all capitals in parenthesis immediately following the title.

4. **DESCRIPTIVE NOTES:** If appropriate, enter the type of report, e.g., interim, progress, summary, annual, or final. Give the inclusive dates when a specific reporting period is covered.

5. **AUTHOR(S):** Enter the name(s) of author(s) as shown on or in the report. Enter last name, first name, middle initial. If military, show rank and branch of service. The name of the principal author is an absolute minimum requirement.

6. **REPORT DATE:** Enter the date of the report as day, month, year; or month, year. If more than one date appears on the report, use date of publication.

7a. **TOTAL NUMBER OF PAGES:** The total page count should follow normal pagination procedures, i.e., enter the number of pages containing information.

7b. **NUMBER OF REFERENCES:** Enter the total number of references cited in the report.

8a. **CONTRACT OR GRANT NUMBER:** If appropriate, enter the applicable number of the contract or grant under which the report was written.

8b, 8c, & 8d. **PROJECT NUMBER:** Enter the appropriate military department identification, such as project number, subproject number, system numbers, task number, etc.

9a. **ORIGINATOR'S REPORT NUMBER(S):** Enter the official report number by which the document will be identified and controlled by the originating activity. This number must be unique to this report.

9b. **OTHER REPORT NUMBER(S):** If the report has been assigned any other report numbers *(either by the originator or by the sponsor)*, also enter this number(s).

10. **AVAILABILITY/LIMITATION NOTICES:** Enter any limitations on further dissemination of the report, other than those imposed by security classification, using standard statements such as:

(1) "Qualified requesters may obtain copies of this report from DDC."

(2) "Foreign announcement and dissemination of this report by DDC is not authorized."

(3) "U. S. Government agencies may obtain copies of this report directly from DDC. Other qualified DDC users shall request through _____."

(4) "U. S. military agencies may obtain copies of this report directly from DDC. Other qualified users shall request through _____."

(5) "All distribution of this report is controlled. Qualified DDC users shall request through _____."

If the report has been furnished to the Office of Technical Services, Department of Commerce, for sale to the public, indicate this fact and enter the price, if known.

11. **SUPPLEMENTARY NOTES:** Use for additional explanatory notes.

12. **SPONSORING MILITARY ACTIVITY:** Enter the name of the departmental project office or laboratory sponsoring *(paying for)* the research and development. Include address.

13. **ABSTRACT:** Enter an abstract giving a brief and factual summary of the document indicative of the report, even though it may also appear elsewhere in the body of the technical report. If additional space is required, a continuation sheet shall be attached.

It is highly desirable that the abstract of classified reports be unclassified. Each paragraph of the abstract shall end with an indication of the military security classification of the information in the paragraph, represented as *(TS), (S), (C), or (U)*.

There is no limitation on the length of the abstract. However, the suggested length is from 150 to 225 words.

14. **KEY WORDS:** Key words are technically meaningful terms or short phrases that characterize a report and may be used as index entries for cataloging the report. Key words must be selected so that no security classification is required. Identifiers, such as equipment model designation, trade name, military project code name, geographic location, may be used as key words but will be followed by an indication of technical context. The assignment of links, roles, and weights is optional.